

2025

# Osteoarthritis age estimation from three-dimensional surface renderings of computed tomography scans

---

<https://hdl.handle.net/2144/51898>

*"Downloaded from OpenBU. Boston University's institutional repository."*

BOSTON UNIVERSITY

ARAM V. CHOBANIAN & EDWARD AVEDISIAN SCHOOL OF MEDICINE

Thesis

**OSTEOARTHRITIS AGE ESTIMATION FROM THREE-DIMENSIONAL  
SURFACE RENDERINGS OF COMPUTED TOMOGRAPHY SCANS**

by

**STEPHANIE L. SHADDOCK**

B.A., Wayne State University, 2021

Submitted in partial fulfillment of the  
requirements for the degree of  
Master of Science

2025

© 2025 by  
STEPHANIE L. SHADDOCK  
All rights reserved

Approved by

First Reader

---

Sean D. Tallman, Ph.D.  
Associate Professor of Anatomy and Neurobiology  
Program of Forensic Anthropology

Second Reader

---

Tara L. Moore, Ph.D.  
Professor of Anatomy and Neurobiology  
Director of Program of Forensic Anthropology

## **DEDICATION**

This work is dedicated to M.I.C. and her plants.

## **ACKNOWLEDGMENTS**

I would like to thank several people for contributing to the creation of my thesis. To begin, my advisors and professors Dr. Tallman, Dr. Moore, and Dr. Pokines for their deep well of wisdom and knowledge. Barbara and Mark Shaddock for endless patience and an unquantifiable amount of support (both monetary and emotional). I would also like to thank Pierre Boucher for the invaluable statistical knowledge he provided to aid in this endeavor. Sandi Mazza for providing her pivotal Excel expertise. Amber Hojnacki and Charles Rini for the desperately needed computer technology advice and aid. Pat and Tom Hojnacki for always encouraging me to stay strong and keep learning. My amazing and supportive cohort of classmates, without whom the completion of this thesis would not have been possible. My friends scattered around MI and NY who provided a vast wealth of inspiration and determination to help me keep moving forward.

# **OSTEOARTHRITIS AGE ESTIMATION FROM THREE-DIMENSIONAL SURFACE RENDERINGS OF COMPUTED TOMOGRAPHY SCANS**

**STEPHANIE L. SHADDOCK**

## **ABSTRACT**

Osteoarthritis (OA) is a joint disease that affects a large segment of the older adult population. Previous studies have been conducted that examine the causes of osteoarthritis, contributing factors, synovial joint biology, and the effectiveness of using new imaging technology in forensic anthropology. Age estimation is used in a variety of methods in forensic cases as a means to aid the identification of an individual. Much of the literature about OA as an age estimation method refers to the potential OA as an indication of age due to the strong link between OA and age. Winburn and Stock (2019) examined OA using an ordinal method to assess the relatedness of OA and age of the individual. The results from Winburn and Stock (2019) suggested OA is a strong indicator of age, so long as the joint is complete and not damaged by surgery or previous injury. While refined OA aging methods have been tested on physical skeletal elements, their utility in medical imaging is largely unknown. The current study aims to apply the method developed by Winburn and Stock (2019) on computed tomography (CT) scans from the New Mexico Decedent Image Database (NMDID). The NMDID is a CT image database consisting of scans of over 15,000 New Mexicans who died between the years 2010 and 2017. Each individual is represented by approximately 10,000 image slices. From these scans, three-dimensional (3D) images will be constructed through the use of DICOM systems, such as OSIRIX-MD. Meshmixer has a multitude of tools and

functions that allow researchers to refine previously rendered 3D models to increase the image's clarity. The 3D images from this study are further refined through the Meshmixer program, which provides a clear render of the images. A joint-age analysis was conducted to provide the information necessary to determine a correlation between OA and age. The results of the current study suggest that OA as a means to estimate age follows the established precedent of other age estimation techniques, even when viewed in 3D-rendered CT scans.

## TABLE OF CONTENTS

DEDICATION .....	iv
ACKNOWLEDGMENTS .....	v
ABSTRACT.....	vi
TABLE OF CONTENTS.....	viii
LIST OF TABLES.....	x
LIST OF FIGURES .....	xi
LIST OF ABBREVIATIONS.....	xii
INTRODUCTION .....	1
PREVIOUS RESEARCH .....	9
Age estimation in forensic anthropology.....	9
Osteoarthritis as an age estimation method .....	19
OA as a disease and related pathology .....	28
NMDID and other programs.....	35
In conclusion.....	39
METHODS .....	41
Scan Selection.....	43
Osirix MD and Meshmixer Methodology .....	44
Extra guidelines and materials used.....	56
Volume v. Surface Render.....	57
Scoring Cleaned Scans.....	59
Statistical Analysis.....	61

RESULTS .....	62
Comprehensive sample analyses .....	63
Sex group results.....	69
Age Group results .....	70
Separate joint analysis .....	72
Intraobserver error analysis .....	74
DISCUSSION .....	76
From the results .....	76
General discussion .....	81
Important Methodology Warnings.....	84
Avenues for future study.....	91
In summation .....	96
CONCLUSION.....	97
BIBLIOGRAPHY .....	102
CURRICULUM VITAE.....	110

## LIST OF TABLES

Table 1. Population Afinity and Age Demographics for Sample .....	42
Table 2. All examined joints and bones.....	63
Table 3. All joints and bones with OA present.....	68
Table 4. All age groups compared to Winburn and Stock (2019) results.....	71-72
Table 5. Cohens Kappa results on intraobserver error.....	74

## LIST OF FIGURES

Figure 1 SR settings in OSIRIX MD. ....	47
Figure 2 SR loading screen in OSIRIX MD. ....	48
Figure 3 Example SR render in OSIRIX MD.....	49
Figure 4 3D render example in Meshmixer .....	50
Figure 5 highlighted unwanted material in Meshmixer.....	51
Figure 6 highlighted wanted material in Meshmixer.....	52
Figure 7. Separate object browser in Meshmixer .....	53
Figure 8 actions dropdownbar (left) and inspector dropdown bar (right).....	54
Figure 9 End product in Meshmixer .....	55
Figure 10 VR example in OSIRIX MD. ....	58
Figure 11 Table 9 from <i>Winburn and Stock (2019)</i> . ....	60
Figure 12 Output 1. ....	64
Figure 13 Output 2. ....	65
Figure 14 Output 3. ....	66
Figure 15 Output 4. ....	66
Figure 16 Left (left) and Right (right) shoulder scatter plots.....	73
Figure 17 Left (left) and Right (right) ankle scatter plots.....	73
Figure 18 personal effects on 3D render.....	86
Figure 19 Pill-bugging. ....	88
Figure 20 cleaned 3D render.....	89

## LIST OF ABBREVIATIONS

3D.....	Three-dimensional
AFAB.....	Assigned female at birth
AMAB.....	Assigned male at birth
AS .....	Ankylosing Spondylitis
BIPOC.....	Black Indigenous Person of Color
BU .....	Boston University
CAD .....	Computer-aided design
CT .....	Computed Tomography
DICOM .....	Digital Imaging and Communications in Medicine
DISH .....	Diffuse idiopathic skeletal hyperostosis
DJD .....	Degenerative Joint Disease
IRB.....	International Review Board
NMDID.....	New Mexico Decedent Image Database
NM-OME.....	New Mexico Office of the Medical Examiner
NOK .....	Next of kin
OA.....	Osteoarthritis
OP .....	Osteoporosis
SR.....	Surface Render
STL .....	Standard Triangle Language or Stereolithography
VA.....	Virtual Anthrpology
VR.....	Volume Render

## INTRODUCTION

Currently, identification methods used in forensic anthropology depend on a few key factors. Often, forensic anthropologists use the biological profile to assist in identifying an unknown individual by focusing on as much descriptive information as possible from the skeletonized remains. When trying to build a biological profile, forensic anthropologists have a set of steps to take to make an estimation that is as accurate as possible. The forensic standards detailed in Langley et al. (2016) are commonly used to collect cranial and postcranial measurements for stature estimation and FORDISC analyses. Forensic anthropologists begin with the determination that the remains are human, modern, and an approximate number of individuals, then estimations of age, sex, stature, and ancestry are explored. There is no stand-alone method that estimates any one parameter of the biological profile; each parameter requires the implementation of multiple techniques and the combination of the results. There is a demand for an age estimation technique that can be consistently relied upon for data collection in some aspects of biological anthropology. Any information that can be used for this process is valuable; however, this proposal will be focused on the area of age estimation methodology.

Age estimation is generally accomplished by analyzing the developmental stages of select bones and associating them with an assigned/chronological age (Boldsen et al., 2021). For example, pubic symphysis phases, iliac auricular surface age estimation methods, dental development stages, and clavicular developmental stages are all age markers that signify a particular age range depending on the stage of development

displayed by the marker (Boldsen et al., 2021; Brooks & Suchey, 1990; Verma et al., 2019). Many existing methods are only relevant to much younger and much older individuals as morphology becomes more varied once humans mature up to around 40 years of age (AlQuatani et al., 2010; Boldsen et al., 2021; İşcan et al., 1984; Scheuer and Black, 2004). The lack of information when it comes to older decedents leaves a gap in identifying individuals in the age range of 40 and above. Identifying individuals in the 60 and above age groups presents its own challenges, as much of this population has pathological conditions and surgical interventions that obscure age identification (Watanabe & Terazawa, 2006). Humans age in a somewhat predictable way that may not be related to pathologies; that is to say, as a species, humans age in an individualistic way. As a result, many age estimation methods have increasingly broader age categories a decedent could be sorted into (Berg, 2008; Brookes & Suchey, 1990; Hartnett, 2010; İşcan et al., 1984). With such broad categories, anthropologists are left with imprecise age estimations only narrowed down through positive identification, which is estimated only after known individuals are compared to the decedent.

As humans age, forensic age estimation becomes increasingly difficult also, as there is a difference between chronological age and skeletal age/development (McCulloch et al., 2017). Chronologic age refers to the socially tracked age associated with several developmental changes, while developmental age refers to the predictable physiological changes that occur as bone matures (Moorrees et al., 1963). When referring to age and age-related phenomena, often the reference is to developmental age; when discussing age estimation methods the reference is to chronological age. Age-related

pathologies are increasingly being used as a means to develop a method to estimate age in older individuals (Alves-Cardoso & Assis, 2018; Brennaman et al., 2016; Listi & Manhein, 2012; Winburn & Stock, 2019). How humans age is often separated by specifically what the researcher has in mind for example, skeletal age v. dental age. Biological age is often divided into skeletal and dental age, as these are two categories that have predictable changes to their structures as they age (Scheuer and Black, 2004).

The study of joint pathologies and their relation to age is an interdisciplinary endeavor, involving knowledge from both medical and anthropological fields. A joint's developmental process is generally known to go through stages of development, growth, and differentiation (Archer et al., 2003). Joint pathologies can arise from any point in this process; however, the age-related changes of OA originate with degenerating cartilage; as the disease progresses, the cartilage is damaged and the surrounding bone becomes affected (Martel-Pelletier, 1999). When assessing living patients for OA, medical doctors will consider physical pain levels, as well as computer tomography (CT) scan analysis of joint and osteological evidence (Burt et al., 2013; Sanchez et al., 2021). When the osteological elements become affected by OA, it can be seen in decedents independent of the presence of cartilage on any of the synovial joints present in the body; this includes those in the spinal column (Brennaman, 2014; Burt et al., 2013). One such study detailed a methodology for measuring OA evidence on body-wide joints, which correlated with different ages (Winburn & Stock, 2019). This methodology scored the temporomandibular joint and all apical joints of approximately 400 modern European-American individuals and ran multivariate analyses to assess for age predictability

(Winburn & Stock, 2019). The sample group used in Winburn and Stock (2019) and the subsequent validation study by Strasheim et al. (2023) used the physical remains from the donated skeletal collection at the University of Tennessee, Knoxville; although the validation addressed variation among the Black, Indigenous, and people of color (BIPOC) within the collection, the fact remains that both studies follow the precedent of using physical human remains for study.

In the digital age, advances in computer scanning technology have made possible the creation of several databases used to aid law enforcement and forensic analysts. Currently, most forensic anthropological studies rely on the use of donated skeletal collections, forensic casework reports, or nonhuman participants (Brennaman et al., 2016; Jurmain and Kilgore, 1995; Pokines et al., 2022). The New Mexico Decedent Information Database (NMDID) offers an alternative to the dry-bone precedent. The NMDID is an online database of human remains that have been collected and stored digitally as a result of several years' worth of research implementing CT and magnetic resonance imaging into the practices at the New Mexico Office of the Medical Examiner (NM-OME) in junction with the University of New Mexico (Berry & Edgar, 2021; Edgar et al., 2020). The free database is a unique resource of full-body postmortem CT scans of over 15,000 individuals along with antemortem health and social information (Vidoli, 2022). Since the NMDID does not formally follow informed consent protocols, the approval of the Institutional Review Board (IRB) is not required in research with the deceased. The NM-OME adheres to its own standards and protocols to protect the privacy of decedents' next of kin and to obtain consent to publish their loved one's information on the NMDID

(Edgar et al., 2020; Vidoli, 2022). The NMDID accomplishes an admirable feat by creating a free, accessible, and credible database for researchers to access from anywhere in the world.

In a similar vein of innovation, the use of three-dimensional (3D) imaging in medical research is increasingly employed. Radiographs and CT scans have been used outside the medical office setting for some time now (Komar, 1998; Malone et al., 2011; Rahim et al., 2020). Medical examiner records are often used in forensic studies; an example is when Komar (1998) used records from the Office of the Chief Medical Examiner in Edmonton to explore decomposition of remains in a cold environment. An example of radiographs being used as the sample study is when Mallone et al. (2011) examined pediatric fracture healing. Where 3D rendered remains are concerned, the methodology includes converting 2D images, such as CT scans, then into 3D images with promising accuracy; when the imaging signal is stronger, the conversions appear more accurately (Buser et al., 2017; Rahim et al., 2020). The aim of using digital mediums in forensic anthropology is not to replace more traditional osteological analysis but to expand on already existing methods and institutions.

The two imaging softwares primarily used in the current study are OSIRIX MD and Meshmixer. OSIRIX MD is a multimodality DICOM viewer that was developed for Mac OS operating systems to be either a standalone or joint function program for viewing medical imagery (Rosset, 2004). With OSIRIX MD, CT scans can be viewed as volume or surface 3D renders and, as was the case in the current study, export the 3D files to other 3D viewing/editing programs. Programs such as Meshmixer, which Buzayan et al.

(2020) used as the means to prepare patient-accurate dental cast models for 3D printing and subsequent use in planning procedures. Meshmixer operates as a free-of-charge meshing program that allows users to isolate sections of large 3D STL files.

Osteoarthritis (OA) is a multifactorial noninflammatory synovial joint disease marked by damage to articular tissue and is also classified as an age-related disease (Burt et al., 2013). A joint is defined as any connection between two or more skeletal elements, while a synovial joint is a joint classification that describes joints coated with a thin layer of hyaline cartilage surrounded by synovial fluid within a fibrous joint capsule (White et al., 2012). This thesis project explores two main points: the first is the use of OA as an aging method on apical joints, and the second is the use of an all-digital sample.

Attempting to assess OA for an estimated age has been applied to other dry bone collections for the purpose of understanding how OA presents and what can reasonably be assessed from its progression (Alves-Cardoso & Assis, 2018; Brennaman et al., 2016; Listi & Manhein, 2012; Snodgrass, 2004; Winburn & Stock, 2019). Since this methodology was based around Winburn and Stock's (2019) study, OA of the spine was not addressed in the current study. It bears stating some verbiage of note for the duration of this document (and especially during the methods section), namely that the words 'files' and 'CT scans' are used interchangeably. This change-up is done because, in the context of these methods, they are essentially the same. The current thesis aims to utilize CT scans and 3D imagery to expand existing research in the topic of assessing OA severity to determine a specific age range for unknown individuals. The definition of a joint as it relates to OA is somewhat disputed even among researchers (Burt et al., 2013).

Age estimation ability greatly depends on the context and integrity of the skeleton elements present (Verma et al., 2019). For the purpose of this study, the glenohumeral (shoulder), acetofemoral (hip), tibiofibular/ patellofemoral/ tibiofemoral (knee), humeralulnar/ humeralradial/ proximal radioulnar (elbow), tibiofibular/ talocrural (ankle), and radiocarpal/ distal radioulnar (wrist) joints were examined postmortem and assessed for OA.

The goal of the current study is to test the effectiveness of OA as an age indicator following the method outlined in Winburn and Stock (2019) on a digital sample of human remains. On the topic of sex, the present study will use the terms assigned female at birth (AFAB) and assigned male at birth (AMAB) to better reflect the current practices of sex examination in forensic anthropology (Kelley and Tallman, 2022). This chapter served as the introduction to the premise of age estimation using OA, as well as the use of 3D-rendered skeletal remains, and introduced several key terms and concepts intended to begin the discourse of the current project. The next chapter will dive deeper into the previous research related to topics such as OA, age estimation techniques, digital anthropology, and several of the programs/databases used in the conduction of this experiment. Chapter 3 will detail the specific methods used to prepare the decedents for participation in this study as well as, collect the data required for analysis. Chapter 4 will serve as the presentation of the collected data and explain how each portion of the data was analyzed. Chapter 5 will further discuss the previous chapter's results, connect those results back to topics mentioned in Chapter 2, delve into study limitations, and explore

launching points for future research. The final chapter will conclude this document with the broad strokes of each chapter and a final statement.

## **PREVIOUS REASERCH**

The inspiration driving the current study revolves around age estimation in forensic anthropology. An essential tool for forensic anthropologists is age-at-death estimation methods for skeletonized remains. The most common methods for broad age estimation include dental development, pelvic analysis, and epiphyseal fusion; and, somewhat less commonly, cranial suture closure, acetabular morphology, and sternal rib end analysis. Pathology has also been used to aid in age estimation. When pathology such as OA is present, it can be used to facilitate age estimation and is noted in forensic casework (Ortner, 2003). Achieving an age-at-death estimation is accomplished using a combination of methods that vary on a case-by-case basis, as human variation is vast. In this chapter, I will discuss age estimation methods, OA, virtual anthropology, and the programs used to complete this project.

### **Age Estimation in Forensic Anthropology**

When estimating the age of an unknown individual it is often helpful to start broadly and work inward, meaning an effective starting point for age estimation is to determine if the individual is juvenile or adult (ie. over or under 18-23 years of age). That knowledge will streamline which methods to employ as some aging methods are better suited to different age ranges. As stated in the introduction chapter, biological age is viewed by the different biological changes that occur when humans age (Scheuer and Black, 2004). The term 'growth' is used to describe progressive changes in size and morphology during the development of a human (Scheuer and Black, 2004). Human

growth is not uniform in all aspects, as it is heavily influenced by environmental and genetic factors (Scheuer and Black, 2004). This is the basis of why humans of the same age may not be in the same stage of growth as each other. The definition of 'age' is often divided into either chronological age or biological age; chronological age is the social age of the individual whereas biological age indicates growth (Scheuer and Black, 2004). Biological age can be separated into the two sub categories skeletal and dental age (Scheuer and Black, 2004). This distinction is made mainly to be precise when discussing topics for research, for example when discussing dental changes with age specifically rather than skeletal differences.

Dental development has been closely studied for the last few decades to create methods for age estimation using teeth structure and development from younger individuals to adults (AlQahtani et al., 2010; Mincer et al., 1993; Lovejoy, 1985; Verma et al., 2019). The current methods rely on morphologic criteria—observed in sectioned or unsectioned teeth—radiological measurements or biochemical readings to estimate an age range in a given individual (Verma et al. 2019). Dental development research is vital to physiological age analysis, as the way human teeth develop occurs in tandem with age (AlQahtani et al., 2010; Moorrees et al., 1963). Dental age can be estimated by the emergence and the formation of the teeth because tooth formation occurs before the tooth emerges in relatively predictable intervals, within specific populations (Moorrees et al., 1963). For example, Moorrees et al. (1963) examined a sample size of 380 juvenile radiographs (161 female and 184 male) total from two different collections; with the goal of detailing at what age different stages of tooth development happens. That study was

able to link crown development, root formation and apical closure to several ages; stating that by the average age of 12 root length was in its mature stage for all teeth with the exception of the third molar (which was only at the crown development stage). Moorrees et al. (1963) found some sex differences with the canine and premolar root maturation, namely that females achieved root development 0.41 to 1.31 years earlier than their male counterparts.

AlQhatani et al. (2010) used a modified version of Moorrees et al. (1963) to explore the variability in tooth formation. AlQhatani et al. (2010) and Moorrees et al. (1963) found consistencies with the notion that tooth formation is least variable in infancy and most variable after the age of 16 years for the development of the third molar. That is to say, identifying the age of infants is more precise than identifying the age of juveniles and young adults through the analysis of tooth development. The result of AlQahtani et al.'s (2010) work is the atlas of human tooth development and eruption, which is commonly used in forensic casework today. AlQahtani et al. (2010) also observed sex differences where females generally mature faster than males, although this was most notable between the ages of 6 and 14; at 15, males third molar mature faster than females. At about sixteen years of age, most tooth development has concluded, with the exception of the third molar, which may develop and erupt between the ages of 16 and 24 years (AlQahtani et al., 2010). Thus the third molars are used more often to determine juvenile remains from adult remains despite being the most varied of the human teeth in terms of shape and symmetry (Mincer et al., 1993). The third molars are examined through radiographs and evaluated for several stages of development, from

crown formation to full eruption with closed apical ends of roots if found present at all (Mincer et al., 1993). If the third molar is present in any of these stages, then the individual is displaying traits consistent with adult remains.

Fusion of osteological structures is also associated with differences in juvenile/young adult age. In order to discuss this method; some background on skeletal growth must be explained. There are two originate forms from which osseous material can grow, endochondral from hyaline cartilage and intramembranous from a highly vascular membrane (Scheuer and Black, 2004). The endochondral ossification gives rise to trabecular bone or cancellous bone whereas the intramembranous ossification results in diploic or dense bones (Scheuer and Black, 2004). Bone develops in stages, first the primary ossification center grows out creating the initial growth cite for each bone (Scheuer and Black, 2004). The initial appearance of ossification centers can also be used to approximate the age of a prenatal or postnatal infant (Scheuer and Black, 2004). Once growth activity has stopped in the growth plate, fusion of the ossification centers begins; where the primary centers stop growing may cause the development of secondary ossification centers (Scheuer and Black, 2004). Epiphyses are the secondary growth centers and they typically form joint surfaces or around areas of strong muscle/ligament attachment (Scheuer and Black, 2004). Epiphyseal fusion occurs at several times during development between the ages of less than 1 year to about 30 years old (Scheuer and Black, 2004).

Common fusion sites that coincide with age are located in the centra of the thoracic and lumbar vertebrae, anterior iliac crest, and the medial clavicles (Albert and

Maples, 1995; Webb and Suchey 1985). In the case of vertebral centra, Albert and Maples (1995) found that no epiphyseal rings were attached before the age of 14 in their female group and before the age of 16 in their male group. Albert and Maples (1995) also found the latest ages at which all vertebrae displayed epiphyseal fusion was 25 in their female group and 24 in the male group. Webb and Suchey (1985) conducted a study on the epiphyseal union stages of the anterior iliac crest and the medial clavicles; stating that epiphyseal union was analyzed in four stages nonunion with no epiphyses, nonunion with separate epiphyses, partial union, and complete union. The results presented by Webb and Suchey (1985) indicate several stages of overlap for both the medial clavicle and anterior iliac crest. For example Webb and Suchey (1985) report for the medial clavicle to exhibit nonunion the individual is 25 or younger if male and 23 or younger if female, partial union indicates 17 to 30 if male and 16 to 33 if female, and complete union indicates an age at or older to 21 if male and at or older than 20 if female. Each development stage overlaps the predicted age ranges of another, resulting in a method that is specialized for the juvenile to young adult age groups.

Moving forward to a different juvenile to adult age estimation method: suture closure analysis. There are two main types of skeletal sutures examined for age estimation: maxillary sutures and cranial sutures (Meindl and Lovejoy, 1985; Mann et al., 1991). Maxillary suture closure analyses conducted by Mann et al. (1991), with a sample size of 186 known individuals, illustrated how suture closure was linked to age as the four maxillary sutures appear to close at a predictable age, and thus could be used to estimate an age range. However, a further validation study found that statistically, the

correlation between age and suture closure is not linear, and that while some success in age estimation is possible with this method (ages 16- 33 can be aged within 15 years) this validation was conducted with AMAB individuals of European population only which differs from the demographics in the Mann et al. (1991) study (Gruspier and Mullen, 1991). Despite its large age groups, suture closure analysis remains effective at estimating the age of juveniles and young adults.

Another form of suture closure analysis examines the cranial sutures, as there is some association to how “open” the sutures on the top of the cranium. Meindl and Lovejoy (1985) examined a sample of 236 crania from the Hamann-Todd Collection with the goal of establishing a cranial suture age estimation method. Meindl and Lovejoy (1985) identified seven points along several cranial sutures and scored their appearance on a 0-3 scale; with a score of 0 indicating the suture was open, 1 indicating the suture is minimal to moderately closed, 2 indicating significant closure, and 3 indicating complete suture obliteration. The results of their study suggest this method was able to approximate age within a 28.6 to 65.4 years of age range, with some notes to the extreme ends of their scale. Namely, the individuals who display fully open and fully obliterated sutures should be aged using other means (Meindl and Lovejoy, 1985). Not every person’s sutures will reach the obliteration stage and some may never even advance past stage 0 (Meindl and Lovejoy, 1985). While the cranial suture closure method is more attuned for adult age estimations, it can be used as a quick method to determine juvenile from adult remains provided suture closure has begun taking place. All of the juvenile age estimation methods become less accurate as the age of the decedent increases. This pattern persists

as it becomes more challenging to distinguish age and variation with time, resulting in large age estimation ranges in the older populations.

In spite of this difficulty, several methods have been developed in anthropology in an attempt to associate a predicted age with an adult individual. Similarly, within bioarchaeology, it has become commonplace to use osteological analyses developed largely for forensic casework and apply them to historical decedents (Huffer 2021). An age estimation method which seriates developmental stages of select diagnostic bones, typically the pelvis, with an associated age range has been applied to paleodemography (Boldsen et al., 2021). Examining skeletal growth can be done to an extent with fragmentary remains; however, the results generally are more accurate with a complete set of remains. New methods are being studied, and one such method involves examining individual bones, assigning a score to them, and taking the sum of the scores to yield an age estimation, called transition analysis (Boldsen et al., 2021). By using the accumulation of multiple bone states, this method adds a layer of information that lends itself to the complex nature of how age and skeletal development are related, which benefits forensic anthropology.

Another area commonly examined for age estimation is the pubic symphysis phases and iliac auricular surface (Berg, 2008; Buckberry and Chamberlain, 2002; Hartnett, 2010; Katz and Suchey, 1986; Lovejoy et al., 1985). Even though the pelvic girdle is most typically associated with assigned sex estimation of a decedent, age estimation methods have been studied for this area and have yielded promising results. Lovejoy et al. (1985) devised a guide to determine adult skeletal age at death using the

auricular surface of the ilium, detailing several descriptive phases that directly correspond to an age range. The result of noted very little sex differences in their sample, and acknowledges that billowing on the auricular surface may persist into later adulthood. With the aim of building from what Lovejoy et al. (1985) detailed, Buckberry and Chamberlain (2002) examined age related features of the auricular surface, scored them individually, and composite scores were made for each individual as a method to predict the age-at-death of an individual. The features used consist of transverse organization, surface texture, microporosity, macroporosity, and apical changes; all of which refer to a region on or near the auricular surface. Since each feature was examined individually the scoring systems were different for each feature and ranged from either 1 to 5 or 1 to 3, with the lower scores more associated with younger ages (Buckberry and Chamberlain, 2002). The results of Buckberry and Chamberlain (2002) indicate that the composite scoring method was more effective at estimating age than the individual scores, and there was no significant difference between AFAB and AMAB groups. The age ranges overlap significantly and are wide to accommodate human variation (Buckberry and Chamberlain, 2002). However, this results in age ranges that are so wide they borderline not being useful; for example, the age range associated with stage IV of Buckberry and Chamberlain (2002) is 29 to 81 years of age. In that case, without other age estimation methods to narrow the predicted age range, a researcher could determine that the individual is adult but not much beyond that.

Still in the pelvic girdle, Katz and Suchey (1986) developed a method using a sample size of 739 AMAB decedents who were between the ages of 14 and 92 from

autopsies performed at the Department of Chief Medical Examiner-Coroner in Los Angeles. Brooks and Suchey (1990) aimed to build from the previous Katz and Suchey (1986) study and formulate an easier to use scale system to estimate age. The resulting method was dubbed the Suchey-Brooks method and is still used in forensic analysis today. The Suchey-Brooks method is assigned sex-specific and breaks the pubic symphysis surfaces into six broad phases of development, which broadly associate to an age group (Brookes and Suchey, 1990). The six phases include: I with billowing of the symphyseal face and lack of delimitation, II with the beginning of delimitation and ridge development may be still occurring, III with the early stages of ventral rampart completion and no bony growths along the margin, IV with a fine grained symphyseal face with a distinct rim that could have bony growths, V with a completely rimmed symphyseal face and potentially a slight depression to the face itself, and finally VI with an irregular face shape and depression that continues as the rim corrodes. Further analysis and testing of the Suchey-Brooks method yielded results suggesting the method may not be completely accurate when estimating skeletal age-at-death, and especially not when the individual is older than 40 (Hartnett, 2010). A modified version of the Suchey-Brooks method where a seventh phase is added to the previous phase options allows anthropologists to place individuals into later morphological phases, and thus be more accurately aged (Berg, 2008; Hartnett, 2010). Pubic symphysis study, like dental analyses, becomes less accurate with increasing age if the decedent becomes older; however, only pubic symphysis estimations become less specific once the individual's age reaches into the fifties- sixties range.

Sternal rib analysis is another age estimation method that is employed by forensic anthropologists when assessing for age-at-death (İşcan et al., 1984). İşcan et al. (1984) has developed an age estimation method that assesses the status of the sternal end of the 4th rib by assessing physiological changes; which relates to a corresponding age range. An assessment of this sternal end rib method has uncovered difficulties when attempting to repeat the study; those being measuring pit depth and accurately adhering to protocol concerning the pit shape, rim, and wall (Fanton et al., 2010). The use of the 4th rib assessment is a valid age method despite the previously mentioned difficulties as a quantitative study showed a link between age at death and the fourth rib (Fanton et al., 2010). Issues of repeatability associated with this method can be attributed to some confusion among researchers as it pertains to the descriptions for each feature change (Fanton et al., 2010). This discrepancy highlights how the description of each stage can use refinement but also provide evidence that sternal rib changes are associated to age at death.

Dentition has been used to estimate adult ages as well as juveniles, however it is not the tooth development that is being examined but wear on the dentition. Lovejoy (1985) found that age correlated with dental wear in a group of people mentioned as the Libbon population due to the consistency in the group's dietary practices and lifestyle. Dental wear is dependent on a consistent diet of high-grit foodstuffs with little to no variation in diet during the time the group occupies a given area (Lovejoy, 1985). The method developed and used by Lovejoy (1985) involves comparing an unknown individual with a range of worn maxillary and mandibular criteria and assigning an age to

the individual based on which phase most closely resembles the decedent. Lovejoy (1985) found the results to be consistent with another previously studied group, a fact argued that shows the regularity of dental wear in humans and thus adds credence to the use of this method. By using this method, anthropologists are uncovering odontological history of past groups and adding to the broader subject of history.

### **Osteoarthritis As An Age Estimation Method**

OA has been used in forensic anthropology as a means of approximating the age of an unknown individual. Only recent studies have tested the limits of how specific an age estimation can be made (Winburn and Stock, 2019; Strasheim et al., 2023). As technology continues to advance, its application to forensic anthropology and analysis of OA has the potential to advance as well. Human skeletal pathology has been studied in a more historical context through conditions like OA. For example, Jurmain and Kilgore (1995) conducted an evaluation of OA in a broader scope by merging forensic data with paleopathological and zooarchaeological data to explore the limitations and interpretations of OA in these contexts. Their study consisted of examining OA using a multisymptom analysis under a paleoarchaeological lens. The results of Jurmain and Kilgore (1995) state that OA has the potential to be used to estimate age as long as some standardization in scoring occurs. Research suggests that the elbow is more prone to mechanical loading than the hip, which is consistent with high rates of OA in the elbows of some groups whose suspected lifestyle involved a great deal of mechanical loading through activities such as hunting (Jurmain and Kilgore, 1995). A limitation of the use of

OA as an age estimator, however, is that studies attempting to refine an age method require the known ages of the individuals present, which is not always possible in historical or archaeological contexts (Jurmain and Kilgore, 1995).

Due to its strong correlation with age, OA has been used in several studies to create a method that aids in estimating age in older individuals (Alves-Cardoso and Assis, 2018; Brennaman et al., 2016; Listi and Manhein, 2012; Snodgrass, 2004; Winburn and Stock, 2019). The scoring system on dry bone developed by Jurmain (1990) has been an effective example of the relationship between OA and age. The scoring system assigns a rating from 0-3 and measures the severity of OA and the presence of osteophytes in synovial joints (Jurmain, 1990). Two clinical scales of note that appear in the literature are the Kellgren Lawrence (K-L) grade and the Osteoarthritis Research Society International (OARSI) Score; however, they pertain more to the clinical diagnosis of OA through radiographs (Klara et al., 2016). The clinical assessment scales are less applicable to forensic cases as the premise for scoring OA relies on pain and joint space assessment, which is not present in dry bone analysis of OA.

The motivation behind Jurmain's (1990) study was to explore degenerative disease changes in archaeologically derived individuals. This study examined lesions present on the joints of individuals from "a prehistoric site on the southeastern side of San Francisco Bay, dating from 500 A.D. up to European contact" (Jurmain, 1990). In order to assess the joints, the author developed a scoring system that assesses the degeneration observed on each of the postcranial joints and the vertebral column. The criteria for the non-vertebral and vertebral joints are slightly different, with the vertebral

criteria being more specific to the overall shape of the vertebrae. In both criteria, the joint is scored on a scale of 0-3, detailing from no evidence of OA to extreme ankylosis (Jurmain, 1990). The specific criteria are as follows: a score of 0 indicates no OA to very slight OA, a score of 1 indicates moderate OA (a raised ridge on the centra and small osteophytes/pitting over less than 10% of the joint surface), a score of 2 indicates severe OA, and a score of 3 indicates ankylosis. Severe OA is defined by Jurmain (1990) as remodeled osteophytes and concave original surface in vertebrae, and also large osteophytes remodeled osteophytes and concave original surface and/or pitting over more than 10% of the articular surface or any eburnation present in the nonvertebral joints. Jurmain's (1990) results demonstrated a correlation between OA and age. The results also indicated significant differences between female and male joint scores, scores between joint types on the same individual, which side of the body the joint was on, and the level of disease progression in the joints (Jurmain, 1990). Overall, this study is consistent with the multifaceted nature of OA and reinforces the connection between age and OA.

Snodgrass (2004) examined sex differences in osteophyte development, specifically in the thoracic and lumbar regions of the vertebral column. The sample size for this study consisted of 384 individuals from the Smithsonian Institution's Terry Collection. Individuals were randomly selected according to sex and age categories, and all individuals were adults between the ages of 20 and 80 years old (Snodgrass, 2004). The author set the criteria for assessing osteophyte scores to follow a 0-4 scoring method, originally created by TD Stewart to assess osteophytosis in the vertebral column (Snodgrass, 2004). The defined criteria are as follows: stage 0 is indicated by the

vertebral central showing no evidence of osteophytosis or formation of a vertebral rim; stage 1 is indicated by minor development of osteophytes, which may be one or two small bony spurs or the beginnings of formations of a vertical rim; stage 2 is indicated by osteophytes that are more defined, larger, or more than two smaller osteophytes, or extensive rim remodeling evident with pronounced lipping; stage 3 is indicated by enlarged osteophytes with severe modeling of the rim and/or formation of a large osteophyte that extends towards the center of the vertebral body or projecting downwards the adjacent vertebra into the intervertebral space; and stage 4, is the most extreme with extensive osteophyte development that extends towards the intervertebral space or the center of the vertebral body but is partially or completely in contact or bridged to the adjacent vertebra (Snodgrass, 2004). In order to examine the relationship between age and osteophyte development, the average osteophyte scores for the thoracic, lumbar, and combined thoracic/lumbar regions underwent separate age regression calculations. The results from the study noted that while both regions can be used to estimate age, the lumbar region showed less variation in osteophyte development than the thoracic and is, therefore, more accurate for estimating age (Snodgrass, 2004). The results also found little variation between the female and male groups used in the study, but the differences that are observed indicate osteophyte scores conducted in this manner have a higher accuracy for predicting age in males than females (Snodgrass, 2004). The conclusion from this result is that females show significantly greater variability in osteophyte stages but that the vertebral column may be used to indicate an age range, nonetheless.

Listi and Manhein (2012) used the William M. Bass Donated Skeletal Collection from the University of Tennessee, Knoxville, and the Donated Forensic Collection from Louisiana State University to assess vertebral OA in relation to age estimation. The 0-4 scoring method, originally created by TD Stewart, was somewhat similar to Jurmain's (1990) scale (Listi and Manhein, 2012). However, this scale differs as it focuses on the amount of lipping present in each joint, defining each score as a scale from least to most lipping. The definitions for each score are as follows: a score of 0 is indicated by no observable degenerative change; a score of 1 is indicated by a slight lipping present; a score of 2 is indicated by moderate lipping; a score of 3 is indicated by severe lipping; and a score of 4 is indicated by ankylosis of adjacent vertebrae (Listi and Manhein, 2012). The Wilcoxon signed-rank test and the Mann–Whitney U-test were used to analyze intra- and inter-observer errors, and the results indicated low inter-observer error at 7.7% and a slightly higher intra-observer error at 19.6% and 24.5% (Listi and Manhein, 2012). The authors concluded that there is a relationship between joint health, degenerative diseases, and skeletal age, as the observed trend was joint space diminished as the ages increased (Listi and Manhein, 2012). One of the goals of this study was to directly establish osteophytes as an indicator of age in vertebral age estimation, but they were unsuccessful. The results of the study left the authors with the general conclusion that vertebral OA alone is not enough information for accurate age estimation (Listi and Manhein, 2012). The inconsistency of the intra- and interobserver changes could be due to the general definitions for each score, as terms such as “severe” and “slight” may not be detailed enough to assign a score.

Brennaman et al. (2016) quantified the correlation between OA and age-at-death estimations of the shoulder using a sample of 206 known individuals of European descent from the W.M. Bass Donated Skeletal Collection at the University of Tennessee, Knoxville, and the Boston University Donated Skeletal Collection. The age range of this sample was 20 to 90 years old and assigned sex was nearly evenly distributed, off by just six individuals. Brennaman et al. (2016) collected data from the glenohumeral and acromioclavicular joints of the shoulder using a modified version of a scoring system developed by Buikstra and Ubelaker (1994) for OA identification. In this modified version, ordinal scores from the prevalence of lipping, surface porosity, osteophyte formation, eburnation, and the estimated percentage of the bone surface area showing these features. Once the initial scoring was complete and a percent score was assigned to each individual, a summation of each was used to conduct statistical analysis between assigned sex, side of the body, and age-at-transition. The age-at-transition estimate, which is the most likely age when an individual would transition between phases, was used to calculate the probability of phase given age (Brennaman et al., 2016). The results of this study indicate this method of age estimation can be used only where all joint surfaces are complete, the left and right sides kept separate, and at least an OA score of 1 present; it becomes less precise once the individual is estimated into a higher age, although this threshold is in the 70+ range rather than the previous 50+ range (Brennaman et al., 2016). This study further supports the idea that OA can be used to estimate age while adding a further challenge that some joints may be more accurate to this than others.

Alves-Cardoso and Assis' (2018) study aimed to provide an age-at-death estimation for older individuals through the analysis of osteophytes. The goal of this study was to achieve further refined age-at-death ranges. The presence of osteophytes might be only pathological, but some argue it is a remodeling response to the abnormal processes occurring with OA and age, linking them all together. The sample size used in Alves-Cardoso and Assis' (2018) study included 603 individuals, with a nearly even division of male and female individuals. The sample collection that was used was the Portuguese Human ID Collections, which houses individuals born between 1822 and 1935 and died between 1891 and 1965 (Alves-Cardoso and Assis, 2018). The age range of the individuals from the sample size was 20 years old to 90 years old. The joints assessed in this study were the shoulder, elbow, wrist, hip, knee, and ankle, and the left and right sides of each were assessed independently of each other. The method used to score and define osteophytes is defined through various stages of lipping, porosity, osteophyte growth, and eburnation. Each criterion was given its own 0 to 4 score, except in the cases of osteophyte growth and eburnation, which operated on a 0-3 score and a 0-5 score, respectively (Alves-Cardoso and Assis, 2018). The scoring method used by Alves-Cardoso and Assis (2018) set clear boundaries for the extent of surface affected on its own 0-3 scale for all the criteria. A score of 0 indicates an absence of skeletal element; a score of 1 signifies less than 1/3 of the joint space affected; a score of 2 signifies if the joint space was affected within 1/3 and 2/3 of the space; and a score of 3 signifies if more than 2/3 of the space was affected (Alves-Cardoso and Assis, 2018). Osteophytes are more associated with age than OA in terms of development patterns, and they display fair

to moderate accuracy when assessed for age in isolation (Alves-Cardoso and Assis, 2018). Despite this, the results found osteophytes are not a good indicator to use for age estimation, although they are age-related and are a good predictor of OA severity.

Most relevant to the present study, Winburn and Stock (2019) took the prevalence of OA and the scoring system by Jurmain (1990) and developed a method to predict an age range for numerous body regions in an individual. The study sample consisted of 408 European-American skeletonized individuals from the William M. Bass Donated Skeletal Collection from the University of Tennessee, Knoxville. The documented information on age, ancestry, sex, height, body mass, occupation, and habitual physical activities was used in the study as a means of sorting the population into test groups for statistical analysis. Ordinal scores of the left and right appendicular and temporomandibular joints were documented following Jurmain (1990) and compared. Winburn and Stock (2019) included elements that showed signs of trauma, pathology, or injury in the study groups to address how these factors play a role in OA and age variation. Once the authors collected the data, a blind study was completed (Winburn and Stock, 2019). Damaged areas on the osteological joint surface were included in the study, but where the joint surface was missing entirely, it was excluded from the final results. The combined joint score was calculated from individual scores summed, and then the sum was divided by each usable element. An age-at-transition analysis was conducted for the earliest age at which OA was present in a given joint and when OA was present for 90% and 95% of their sample. OA was noted for hand and foot joints as present or absent instead of the numerical rating system. Age was not obscured by OA and was found to be a consistent

predictor of OA in nearly all examined joints (Winburn and Stock, 2019). The results indicated that when OA is present, it can be used to refine age estimation, but it was recommended that only complete skeletal remains be used and only joints without surgical intervention or otherwise modification be used (Winburn and Stock, 2019). Winburn and Stock (2019) also expressly indicated that certain skeletal joints are more effective than others at estimating an effective age range, stating the female ankle and male temporomandibular joint should not be used, and the female knee should only be used if necessary.

A validation study of Winburn and Stock's (2019) method was conducted that sought to test population variance using this method on a diverse sample (Strasheim et al., 2023). The methodology followed that of Winburn and Stock (2019), while testing its effectiveness on a more diverse sample (BIPOC individuals from the University of Tennessee's Donated Skeletal Collection); "This served to test whether embodied inequity from lived experiences may preclude the ability of the OA presence/absence method to estimate age at death" (Strasheim et al., 2023). The study sample of Strasheim et al. (2023) was subdivided into two groups for assigned sex (male and female), two groups for population affinity (white and BIPOC), and the authors utilized an age range of 18 to 100 (although the distribution of ages was asymmetrical due to availability). The unequal distribution of demographics in the base collection appeared to be a large factor in how the study sample was organized. This study examined the TMJ, shoulder, elbow, wrist, hand, hip, knee, ankle, and foot joints and marked them as either "OA present" or "OA absent" without knowledge of the donor's demographic data by combining the left

and right scores, averaged them to get a present or absent determination (Strasheim et al., 2023). This study utilized a transition analysis to generate age estimates from the left-right combination scores. This study's results demonstrated that the original methodology was validated, and the approach was accurate at estimating the age-at-death of BIPOC individuals. The findings from this study revealed that the hip and shoulder were highly consistent and reliable and are recommended for use as the strongest indicators of age-at-death, while the TMJ and ankle performed poorly and should not be used for age estimation (Strasheim et al., 2023). This validation study further supports the broad application of Winburn and Stock's (2019) method as a viable means to estimate age of deceased individuals. The Stasheim et al. (2023) study also reinforces the idea that a presence/absence methodology for OA-based age estimation is preferable to one based on degree of severity when dealing with cases of fragmentary or incomplete remains, which is more common for forensic casework and bioarchaeological fieldwork.

### **Osteoarthritis as a Disease and Related Pathology**

Osteoarthritis is a multifactorial disease that targets and reduces the synovial joints in an individual, typically older adult individuals (Burt et al., 2013; Martel-Pelletier, 1999; Ortner, 2003; Waldron, 2009; Winburn and Stock, 2019). OA is a disease that deteriorates the synovial joints of the human body in a gradual progression, affecting chondrocytes (cartilage cells), connective tissue, and subchondral structures (Martel-Pelletier, 1999). While there are a variety of initial causes of OA, the pathogenesis appears the same: loss of homeostasis at the cellular level exacerbated by increased joint

friction due to age, resulting in cartilaginous and subchondral bone change (Burt et al. 2013). Joint deterioration occurs over time due to repeated use and other intrinsic and extrinsic factors that break down the protein and carbohydrate-rich connective tissue that fills the space between cells, also known as the extracellular matrix (Burt et al., 2013). As the cellular matrix breaks down, the fissures cause ulcerations to form, and the original joint surface thickness lessens while simultaneously, bony projections (osteophytes) form, and the subchondral layer thickens (Martel-Pelletier, 1999). The result is a warped joint surface, altered from its original shape, complete with osteophytes along the joint margins and, in some cases, complete joint fusion (ankylosis). OA presents in live humans often as painful sensations to the affected joint that prompt the person to seek medical attention. The medical assessment of OA is centered around pain, although people have been diagnosed through the narrowing of joint space on radiographs (and report no pain), stiff swelling around the joint, limited range of motion, weakness in the muscles around the joint, and occasionally joint instability (Burt et al., 2013). OA presents on skeletal remains in roughly four stages of progression once the subchondral layer begins to thicken; slight OA, moderate OA, severe OA, and ankylosis (Jurmian, 1990). In the case of other degenerative diseases, a person typically has diminished bone density, which is indicated as a factor; generally, it seems OA has the opposite effect (Sezer et al., 2010). The duality of OA is that the disease is both destructive and proliferative; the original composition of the joint is initially broken down, and then the underlying structures become thicker and branch out into the joint space.

Despite in-depth research attempts to better understand OA, its specific cause is unknown (Archer et al., 2003; Dahaghin et al., 2005). However, there are known factors that contribute to the progression of the disease. Some known factors include age, weight, family history, and sex (Dahaghin et al., 2005). Some research suggests that trauma plays a role in the severity, activation, and progression of OA, as trauma is also an associated risk factor (Gilmour and Plomp, 2022; Guilak et al., 2018; Shane Anderson and Loeser, 2010). However, the amount of influence each factor has on disease appearance is an area of pathological research that requires further study. For example, some results support that hand OA represents a risk factor for the development of either or both hip and knee OA later in life (Dahaghin et al., 2005). OA is the most prevalent joint disease and a leading source of chronic pain and disability in the United States and manifests itself in a variety of ways; knee OA alone affects at least 19% of American adults aged 45 years and older (Wallace et al., 2017). OA is diagnosed in clinical settings through the use of CT scan evaluation and pain assessments (Klara et al., 2016). OA can be observed on CT scans through visual evidence of lipping around joint elements and narrowing cartilage spaces (Mathiessen et al., 2016). OA presents in joints with multiple degrees of severity, which can be measured and ranked based on the degree of disease progression. The nature of OA is both highly studied and lacking nuance, as it is an extremely complex disease that has detrimental effects on the joints of a person. For as much as researchers do know about OA, more research is necessary to understand its complexities (Dahaghin et al., 2005; Guilak et al., 2018; McCulloch et al., 2017).

A common issue that arises when evaluating OA (in a forensic context) is that its appearance may be confused with other commonly seen pathological conditions. OA is proliferative; however, several diseases that present similarly are erosive, such as osteoporosis, diffuse idiopathic skeletal hyperostosis, and ankylosing spondylosis (Waldron 2009). General degenerative joint diseases and conditional fusing of the carpals may also be confused for OA or may occur alongside developing OA. Also, due to the nature and progression of these conditions, many of these conditions can affect how and if others develop in the same individual. This segment explores other pathologies that are similar to, and as a result may be confused for, OA.

Osteoporosis (OP) is another age-related disease; however, the exact nature of its relationship to OA is unknown (Tarantino et al., 2014). OP causes a reduction of bone mass and quality, which creates a high fracture risk (Tarantino et al., 2014). Despite also being an age-related disease, OP does not commonly exist with OA, which is thought to be due to the reductive nature of OP compared to the proliferative behavior of OA (Sezer, 2010). The most glaring difference between OA and OP is that both affect the skeleton differently at the cellular level. Macroscopically, OP can be distinguished from OA via the degree of porosity and trabecular thickness of the affected element. OP-affected elements present with diminished trabecular bone and increased porosity, occasionally to the point of structural weakness (Adejuyigbe et al., 2023). In contrast, OA has the opposite effect, presenting with osteophytes and increased subchondral bone density. Although joint pain is sometimes associated with OP, OP can occur throughout the

human skeleton and is, therefore, not limited to joint spaces in the way OA is (Sezer, 2010).

Diffuse idiopathic skeletal hyperostosis (DISH) is a condition that results in the ankylosis of the spine via ossification of spinal ligaments and is diagnosable over radiographs or observed in skeletonized remains (Aufderheide and Rodriguez-Martin, 1998). DISH occurs without the development of intervertebral disk disease and does not involve cartilage or synovium of the spine (Aufderheide and Rodriguez-Martin, 1998). The most recognizable characteristic of DISH is the ‘candlewax’ appearance the condition creates when the anterior longitudinal spinal ligament ossifies, creating a dense structure down the length of the spine that does not vary much in size.

Ankylosing spondylosis (AS) is a progressive disease that involves the spine, sacroiliac, and other major joints. AS has an end result of calcification of not just the ligaments but also the joint surface structures, the process of AS development is as follows: initial inflammation followed by granulation of tissue and joint surface erosion, which leads to fibrous tissue healing that leads to calcification which produces ankylosis (Aufderheide and Rodriguez-Martin, 1998). AS is distinguishable from DISH in a few ways; AS is seen in other joints, not just the spine; DISH usually has a later onset time period, and AS involves the ligaments of the joint and the joint surface. Both AS and DISH are distinguishable from OA in that OA creates changes for only the joint surface and not the surrounding tissue.

Degenerative joint disease (DJD) is a general term that describes several conditions, such as apophyseal degenerative disease, osteophytosis, and intervertebral

disk hernia (Aufderheide and Rodriguez-Martin, 1998). DJD has two major classifications, primary and secondary, where primary or idiopathic has no apparent cause, and secondary is caused by a traumatic event or circumstance (Aufderheide and Rodriguez-Martin, 1998). DJD can be indicated on radiographs via diminished joint space and often affects the weight-bearing lower extremities before other joints in the body (Aufderheide and Rodriguez-Martin, 1998). Of the listed conditions, osteophytosis has the most entangled history with OA; this is because osteophytosis has a nearly identical criterion to OA in that osteophytosis is the development and growth of osteophytes (Siebelt et al., 2015). Two core features differentiate the two conditions: eburnation and osteophytosis. Eburnation is seen exclusively in OA and is considered pathognomonic of OA on skeletal remains, and osteophytosis occurs in apophyseal joints, such as the vertebral column (Ortner, 2003). In the literature that studies the vertebral column, OA and osteophytosis are used almost interchangeably since they are often seen together on the vertebrae (Listi and Manhein, 2012; Ortner, 2003; Snodgrass, 2004). Despite their history and likeness, osteophytosis and OA are not associated with each other in the vertebrae (Listi and Manhein, 2012). While DJD and especially osteophytosis are similar to OA, there are enough distinguishing differences between the conditions to study them separately.

It was mentioned earlier in this chapter how a common cause associated with OA is sustaining prior joint injuries. If a person sustains a fracture, near a joint or the fracture extends into a joint, it is almost certain that OA will eventually develop unless the original anatomy can be restored via surgical intervention (Waldron, 2009). Previous

injury to a joint (e.g., torn rotator cuff, car crash damage) not only contributes to the progression of OA but can be mistaken for early OA development (Waldron, 2009). If an antemortem fracture is not mended, the resulting deformity will impact joint use, and the individual will likely develop OA (Waldron, 2009). If the patient becomes a decedent in the interim, and the healed deformed fracture is near the joint itself, it is possible for anthropologists to confuse the two maladies.

Carpal skeletal disorders may mimic advanced OA, such as the medical condition known as lunotriquetral coalition (LTC). As mentioned in Winburn and Stock (2019), LTC has been confused with ankylosis in previous studies. Despite LTC appearing as if the lunotriquetral joint has ankylosed, LTC is in fact, a separate phenomenon where the lunate and triquetral (of one or both upper extremities) are essentially fused to such a degree that the carpals appear as one mass of bone (Mertens et al., 2023). The process by which this occurs is what differentiates LTC from ankylosis, as LTC is a form of developmental variance where the separate carpals fuse during growth and development. A case study of nine individuals highlighted the varying classes of joint coalition; some cases involved surgical intervention to alleviate pain associated with LTC (Ritt, 2001). Winburn and Stock 2019 warn against confusing LTC with ankylosis as they are not the same phenomenon, and LTC has no discussed/tested link with OA.

### **NMDID and Other Programs**

As mentioned in the previous chapter, The NMDID is an online database of human remains that have been digitally stored and collected as a result of a multiyear research implementation of CT and magnetic resonance imaging into the practices at the NM-OME in cooperation with the University of New Mexico (Berry and Edgar, 2021; Edgar et al., 2020). The entirely free database is a unique resource of full-body postmortem CT scans of over 15,000 individuals along with antemortem health and social information (Vidoli, 2022). That is to say, the NMDID records the life data for each decedent and stores that data with the associated medical images on a digital file. Each decedent is organized via a six-digit number corresponding to the filing system used by the NMDID (Edgar et al., 2020). The NMDID search engine allows users to enter different criteria to inquire about the case file of the decedent they are looking for. The search criteria consist of demographic information, pregnancies, location, medical history, physical characteristics, social environment, cause/manner of death, and cadaver environment; if a researcher already has an identification number of a decedent, that number can be searched for as well (Edgar et al., 2020). All of the information associated with a decedent was collected from the medical examiner, family or medical records (Edgar et al., 2020). For example, population affinity is recorded in NMDID in a few ways, namely through the NMDID-organized categories of either race or ethnicity and then further for both categories, the next of kin (NOK) reported race/ethnicity or the medical examiner reported race/ethnicity. When a search is put through the system, files will appear with case identification numbers. Opening these files will give a preview of

all of the information associated with that individual, along with radiographs of the individual. The scout images, as the radiographs are referred to, are meant to serve as a fast preview of the quality of the other forms of medical imaging for that individual. Once decedents are selected, the researcher has to go through a vetting process to ensure the remains are being studied, and then the decedent's file can be downloaded (Edgar et al., 2020).

Many programs have been designed which convert a 2D image to a 3D model by mapping landmarks in X, Y, and Z coordinates (Fruciano, 2016; Stachowiak et al., 2016). Still, as with all methodology, there is a margin of error to account for called digitization error, which is defined as the error calculation caused by the 2D to 3D image change (Stachowiak et al., 2016). Digitization error is typically low, provided the information entered into the digitizer is accurate (Fruciano, 2016). Often the external surface of an object, rather than the volume, is all that is required for a 3D image study; in this case, surface topography can be isolated and visualized as 3D polygon mesh (Landi and O'Higgins, 2019). In recent years, programs have been developed that allow 2D images to be rendered in 3D in Digital Imaging and Communications in Medicine (DICOM) viewers. Examples of DICOM viewers are programs like OSIRIX series and RadiAnt. Kochhar et al. (2021) evaluated intra and inter observer accuracy when examining maxillary volume measurements and the effect of side on the reliability of maxillary volume evaluation using OSIRIX MD. The results from Kochhar et al. (2021) indicate that although a clinical difference in volume assessment was observed, the differences were statistically insignificant. OSIRIX software was utilized to measure the osteological

elements and when examined, the software was able to provide good reliability in measurements of bone volume (Kochhar et al., 2021). For the current study the surface render function of OSIRIX MD will be used to render surface scans and export them as STL files for joint isolation.

Secondary programs are often used in these cases to refine the 3D images formed by DICOM viewers. Adams and Otárola-Castillo (2013) advocate for the use of the program *Geomorph*; which is a package for statistics in R that allows geometric morphometric shape analysis in the digital space. Meshmixer is another example of a secondary program and can be used to upload the 3D rendering and refine the image even more, resulting in a clean 3D image that can approximate the osteological elements more than the rendering alone can. The benefit of using 3D imagery that is scaled to realistic dimensions. Meshmixer will be used for the secondary program for the current study as it can be used to create accurate 3d printable models from scanned biological material (Buzayan et al. 2020). Kelley and Tallman (2022) also used Meshmixer, as well as OSIRIX MD, to organize and formulate their data, and applaud both programs' speed and accuracy.

Landi and O'Higgins (2019) delve into detail about the various imaging techniques that have been employed when studying human biology. Of the methods mentioned, CT scanning technology was among the most versatile, and offered a range of conduction methods. Micro CT scanning operates on smaller scales and has an even higher resolution than CT scans; however, this comes at a large monetary cost comparatively (Landi and O'Higgins, 2019). In medicine, CT scanning is preferred for

osteological analysis but has limitations when it comes to personal effects that may skew the resulting image (Landi and O'Higgins, 2019). Despite the limitations, CT scan data can and has been used for the last twenty years at least to conduct medical analyses. Kurenov et al. (2015) used patient medical information to create 3D renderings for the purpose of medical surgical planning on the throat/chest region. The methodology is similar to that used in the current study where CT scans were collected and processed through digital processors (different from those used in this study) and then formulated into a 3D model that is further printed into reality. Kurenov et al. (2015) further attest that it is feasible to create 3D models that could be useful for a variety of surgical needs, and then explain how the chest region was an example format when in actuality this technique can be used for structures all around the human body. Franklin et al. (2016) discusses the term *virtopsy*, a virtual autopsy, and is a prime example of a benefit of digital applications to remains. A *virtopsy* describes the use of non-invasive medical imaging such as CT scans, radiographs and sonography to conduct an autopsy without cutting into the actual remains. Initially the concept of a *virtopsy* was brought for religious objections to the traditional autopsy, however today it has the potential to broaden the ease of learning and expand student experience working with real human remains.

As technology becomes more advanced, scientists continue to explore the limits of technological use in clinical and academic research. The field of anthropology is no exception to this, as made evident by a small formation of the subfield deemed 'virtual anthropology'. Virtual anthropology (VA) is defined as an interdisciplinary approach to study human anatomical data, along with human ancestors and close evolutionary

relatives in three or four dimensions (Weber and Bookstein, 2017). Essentially VA is the use of advanced computer technology to conduct quantitative analyses within the various fields of biological anthropology. While CT scans, MRIs, and radiographs are more commonly associated with clinical assessments, they also provide a clear set of starting data for studies within VA. From CT scans, both volume and surface renders can be created to analyze a myriad of different topics (Weber and Bookstein, 2017). Advanced computer programs that take two-dimensional (2D) images and render them into 3D models are vital to this process, such as the methodology of Kelley and Tallman (2022) which used CT scans converted into 3D surface renderings to estimate assigned sex-at-birth under a population-inclusive model. The aim of Kelley and Tallman (2022) was to test the accuracy of population-inclusive models in relation to population-specific models. The results of their study not only support the use of population-inclusive models but also show that 3D imaging can be used to reflect sexual dimorphism accurately.

### **In Conclusion**

All of the themes discussed within this chapter add up to the current study about age estimation using OA and 3D rendered human remains. Forensic anthropologists rely on age estimation methods when attempting to identify an unknown individual. While there are several factors that influence OA, age stands out as one of the most prominent and thus OA has been used to estimate age. CT scans and other forms of medical imaging already provide a great use to the medical field, but they have the potential to be implemented even more in forensic research. The NMDID presents an amazing

opportunity to examine a modern population of decedents through medical imaging, namely CT scans. DICOM viewers allow the CT scans to be transformed into 3D models that can be analyzed digitally. The specific methods of the current study and more information about the programs used in the current study will be proposed in the following chapter.

## METHODS

This project is meant to serve as a test point for the use of digital remains in forensic study, using the method explained in Winburn and Stock (2019) to estimate the descendants' age. This project will succeed in the first aim by using CT scans downloaded from a real-world decedent database as the study sample, and the second by comparing the results of Winburn and Stock (2019) to the results of the current study. This will be accomplished by isolating several main joints from a sample size acquired from the NMDID. The NMDID records life data for each of the decedents and stores it with the associated medical images; this is what is called the metadata for each individual. The joints examined in this project are the shoulder, elbow, wrist, hip, knee, and ankles. In order to assess these joints for OA, each bone was scored individually: the glenoid fossa of the scapula, proximal humerus, distal humerus, proximal radius, proximal ulna, distal radius, distal ulna, lunate, scaphoid, acetabulum, proximal femur, distal femur, patella, proximal tibia, distal fibula, distal tibia, and talus. The combined scores from each element were recorded along with the individual scores. This data was then used to see how well the Winburn and Stock method held up on 3D-rendered remains.

The study sample: The original sample used for this project includes full-body CT scans of about 350 individuals, of which only 150 were used as the ultimate sample study for this project. Age cohorts consist of seven total groups: 20-29, 30-39, 40-49, 50-59, 60-69, 70-79, and 80+. The two sex cohorts used in the current study consist of assigned females at birth (AFAB) and assigned males at birth (AMAB) individuals. The male

group consists of 73 individuals, and the female group is represented by 77 individuals. While population affinity was not a tested factor in the current project, the population affinity of the current sample was constructed to utilize a variety of backgrounds since the NMDID provides access to a diverse sample pool. The population affinity for the project sample is represented by the five major American-biased demographic ancestry groups: Asian American, African American, Latin American, Native American, and European American. The direct numerical breakdown of this sample's age and population affinity can be seen in table 1.

Age Group	Number of Decedents (age)	Population Affinity	Number of Decedents (population)
20-29	22	Native American	34
30-39	23	African American	27
40-49	19	European American	57
50-59	27	Latin/Hispanic American	11
60-69	25	Asian American	21
70-79	15	N/A	—
80+	19	N/A	—

**Table 1.** Population affinity and age demographics for sample.

### **Scan Selection**

The CT scans used were acquired using a random sample of individuals from the NMDID. The selection is not completely random as participants were chosen by criteria of equal females and males of specific age groups and population affinities. However, once the criteria were entered into the NMDID search engine, a random number generator (input with the total number of results) was used to determine which individual was chosen for inclusion. At this stage, only radiographs of the individual being viewed were available for evaluation. Each individual's radiographic images were screened for visual legibility and completeness. Individuals were excluded if their images were incomplete, they were missing elements of a joint, or they had a surgical intervention on one or more joints. Population diversity was also considered when choosing individuals by incorporating the five major American-biased demographic ancestry groups: Asian American, African American, Latin American, Native American, and European American. The categories listed from the search engine on the NMDID website do not directly follow this organization method, so for this project, the method outlined in Kelley and Tallman (2022) was implemented. The categories African American, European American, and Native American have corresponding "race" criteria within the NMDID: Black or African American, White, and Native American without tribal specification, respectively. The Asian American group was constructed from the multiple NMDID "race" categories of Chinese, Filipino, Japanese, Korean, Vietnamese, and "other Asian" because these groups individually do not have a large enough representation within the database compared to the other population affinities (Kelley and

Tallman, 2022). A similar approach was taken with the Latin American group by selecting both Hispanic and Latino ethnicities (Kelley and Tallman, 2022). To ensure no cross-listing between categories, an additional ethnicity will be selected as “Not Hispanic, Latino, or Middle Eastern” for all population groups, excluding Latin American (Kelley and Tallman, 2022). There are two other categories listed on the NMDID website, titled “other” and “unknown”; however, for the purposes of this study, these categories were omitted entirely from the selection. When each information file was downloaded, the computer files were downloaded to organize the files by case number, an arbitrary six-digit number corresponding to the filing system used by the NMDID (Edgar et al., 2020). The age, sex, and population affinity were recorded along with the coded identification number and the NMDID identification number in an Excel sheet (for organizational purposes).

### **OsirixMD and Meshmixer Methodology**

Once the full body scans were acquired and downloaded, the images were converted through the OSIRIX MD DICOM program. This process was primarily dictated by trial and error method as the current standard for publication appears to be to state only the name of the program used, not how it was used. For this project, the following standard was implemented: 10 files were uploaded to OSIRIX MD at a time, and then when one was ready, the image file for the ‘head and shoulders’ was selected. The load time to upload the scans this way was a range of thirty minutes to an hour (to upload all 10 completely); however, once a scan was uploaded, it could be opened while

the rest continued in the background. There are two viewing options to choose from, a thin st and a bone st, i.e. the predicted settings that allow the CT results to be viewed at different intervals, thus making the image slightly more or less detailed. While the bone st had somewhat more legible results, the resulting STL file size was much larger and took more to open in MM. The thin st meanwhile ran the risk of textural issues, but when usable, the thin st file type could open comparatively faster and have smaller file sizes. Both file types were used during this project with a preference for the thin st where possible. From there, a surface render was created using the '2D/3D' drop-down menu, which prompts a small screen displaying the render settings. These settings allow the user to alter the surface render qualities manually. There was some variation in the use of these settings as the preset configuration yielded unusable results. An example of a typical SR setting configuration for this project is: high resolution, pixel value of 0.48, decimate value of 32, and smooth iterations of 246. These values came about through several weeks of trial and error where the author would change one setting at a time, allow the image to render, and evaluate for legibility. These values are also not standard across the entire sample as each scan required different settings to achieve optimal legibility, however the values were used as the starting point to evaluate each scan. The time range it took to render each scan was anywhere from fifteen minutes to three hours with the most common render time as roughly an hour on the 32GB MacBook. When the render finishes, it is examined for joint completeness and visibility; as long as the joint surface is at least 80% visible, the image is deemed acceptable for use, following the recommendation from Streishem et al. (2023). The CT file was then exported as an STL

file to one of the external hard drives. Once the first ten files had moved through OSIRIX MD, ten more files were uploaded, and the process was repeated until the decedents had all been processed.

Once the OSIRIX MD files have been saved in a different format, they are ready to be imported into Meshmixer. In OSIRIX MD there is a built-in function where the rendered SR could be imported to MM immediately; however, this extended the render time and altered the render hue of each SR (it made the virtual bones blue in a way that could not be changed once imported). Upon importing the images into Meshmixer, the joints must be isolated from the rest of the image. This consisted of digitally carving away portions of the render, leaving only the desired joint, see **Figures 1-9**. provide visual example of the major steps taken to process the individuals through both Meshmixer and OSIRIX MD.

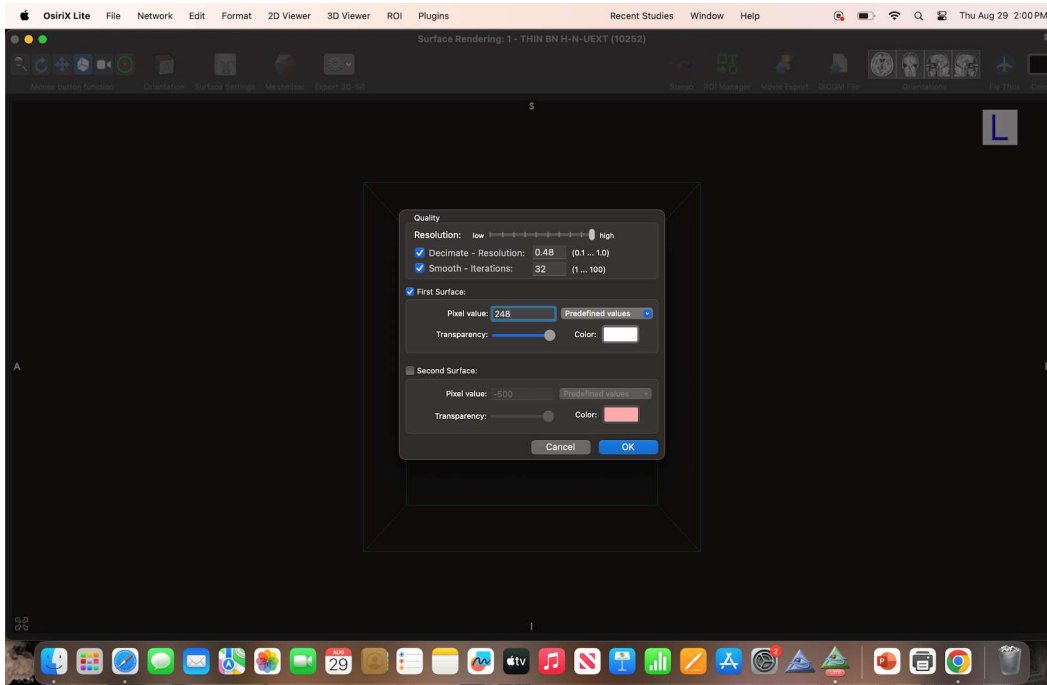


**Figure 1.** SR render settings in OSIRIX MD. Each setting is set to the settings used the most during the processing phase.

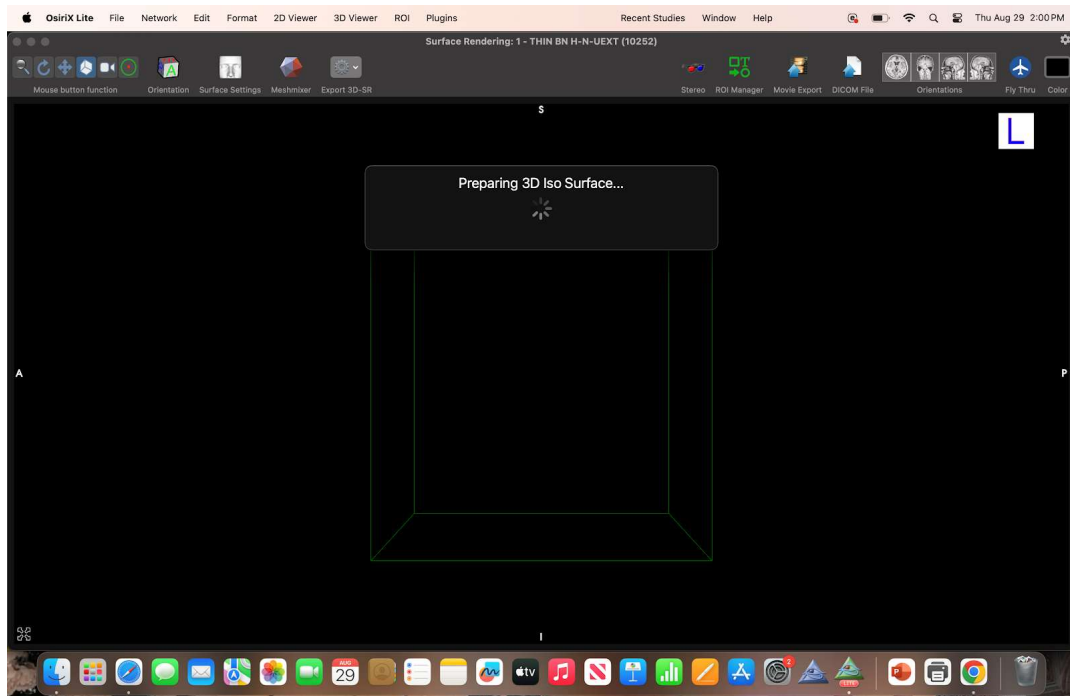


**Figure 2.** SR loading screen in OSIRIX MD. This is the next screen after the render settings. This loading could take as short as five minutes and as long as several hours.

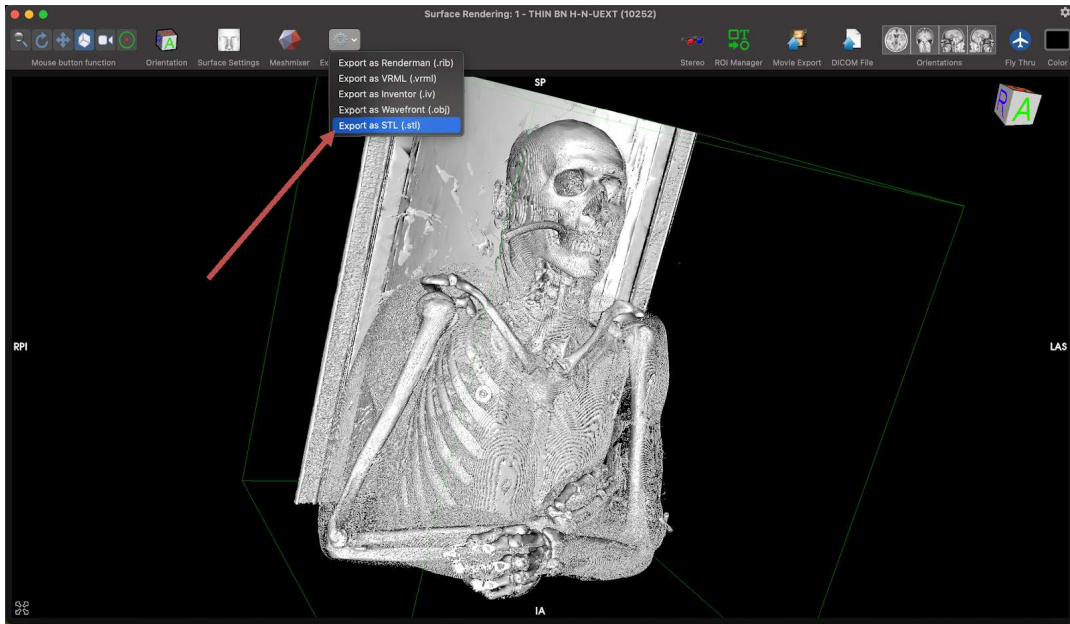


**Figure 3.** Example SR render in OSIRIX MD. After examining the scan for joint completeness, this image is exported as an STL file via the export drop-down menu (red arrow) and stored on the external hard drive (not shown).

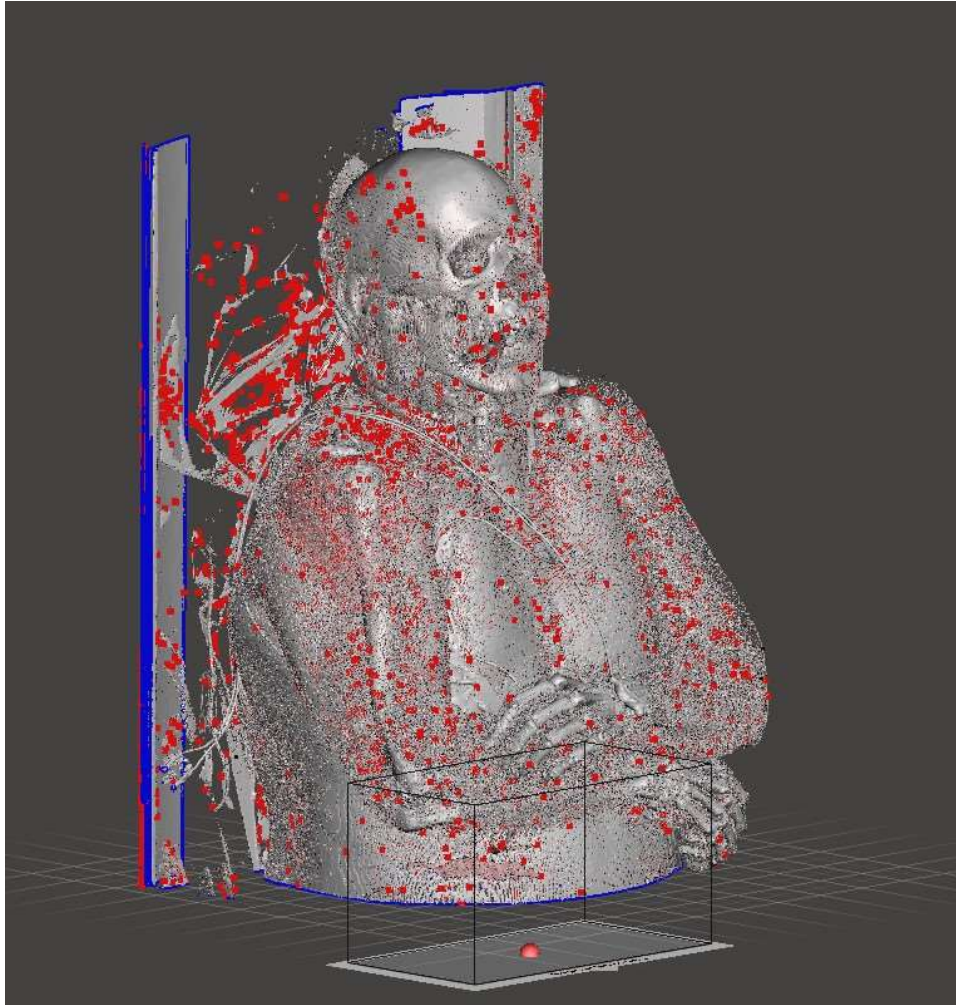


**Figure 4.** 3D render of the example individual in Meshmixer. Individual is shown pre-processing, as they would be upon initial import to meshmixer.

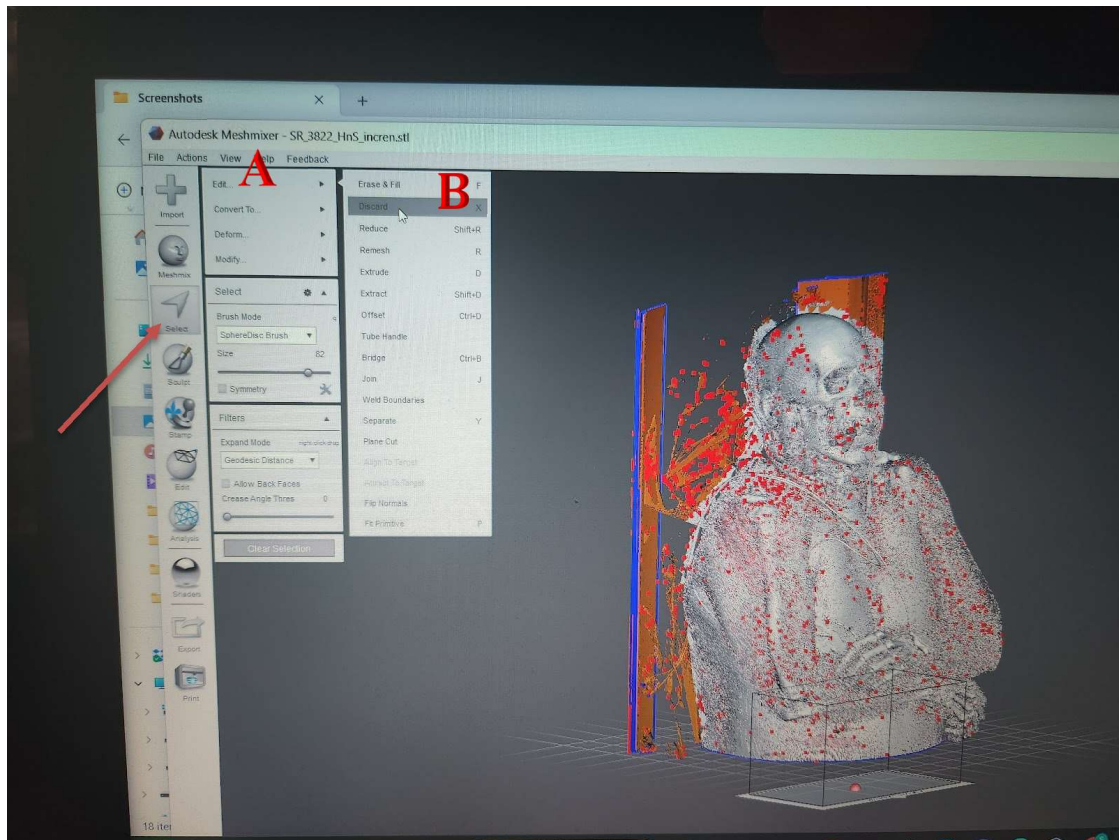


**Figure 5.** Highlighting unwanted material in Meshmixer. Once the select button is engaged (red arrow) the user can move their cursor and highlight unwanted material. Once highlighted, the user can discard this material by selecting edit (A) and then discard (B).

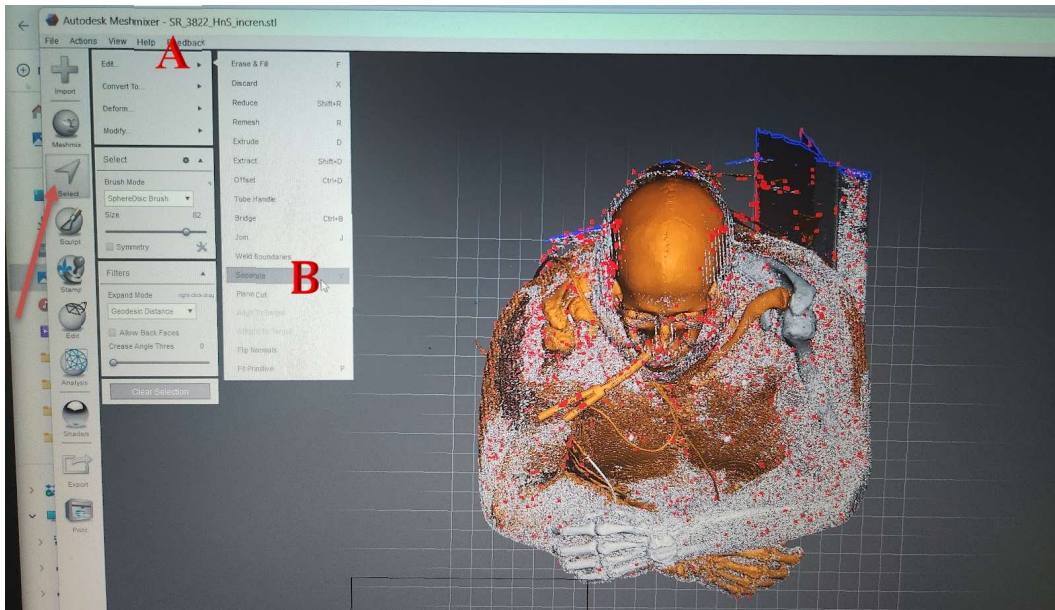


**Figure 6.** Highlighting wanted material in Meshmixer. Similar to how one would discard material, wanted material could also be highlighted and saved separately. Engage the select button again (arrow), highlight the material needed, select edit (A) and then select Separate (B).



**Figure 7.** Separate object browser in Meshmixer. Once the separation occurs, meshmixer views the highlighted region and the non-highlighted region as two different entities. The object browser will appear on the right lower corner of the screen to indicate this. From here, users can click on the part they do not want to keep and delete it via the delete button (arrow).

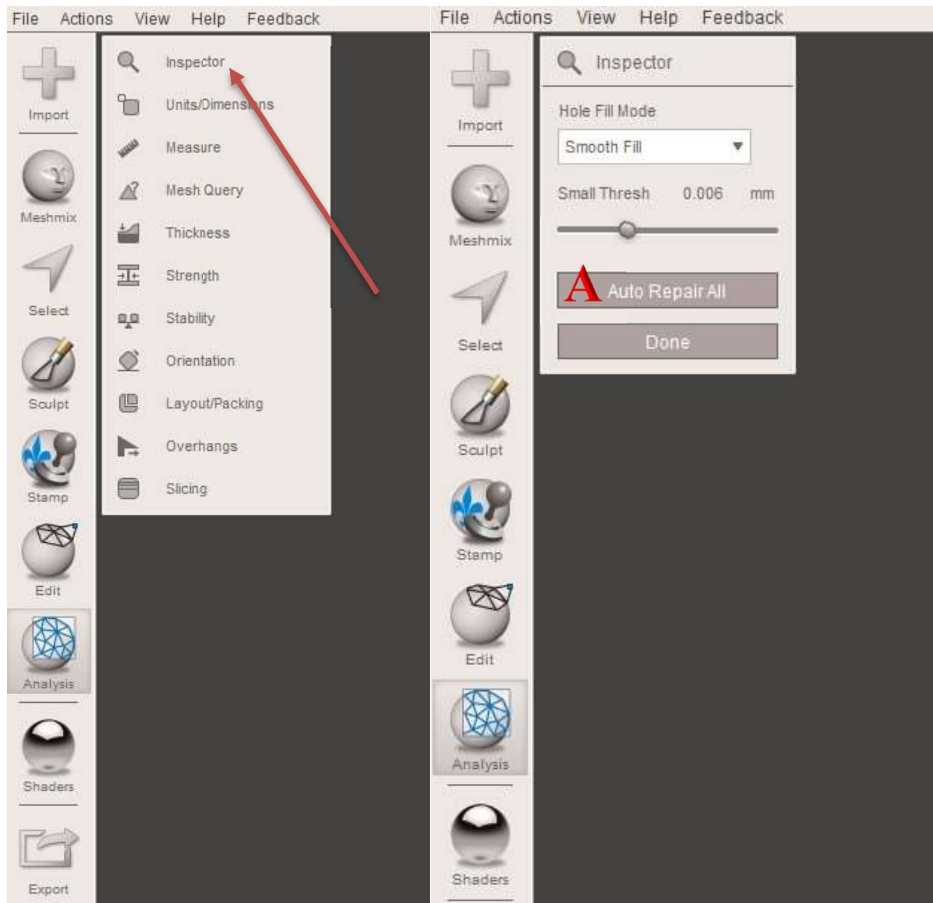


**Figure 8.** Actions drop down (left) and Inspector tool drop down (right). Once most of the unwanted material is gone, what is left can be reduced using the inspector tool (red arrow). The dropdown menu displays settings used in the current study. Use the Auto Repair All button (A) when there are many errors in the mesh.

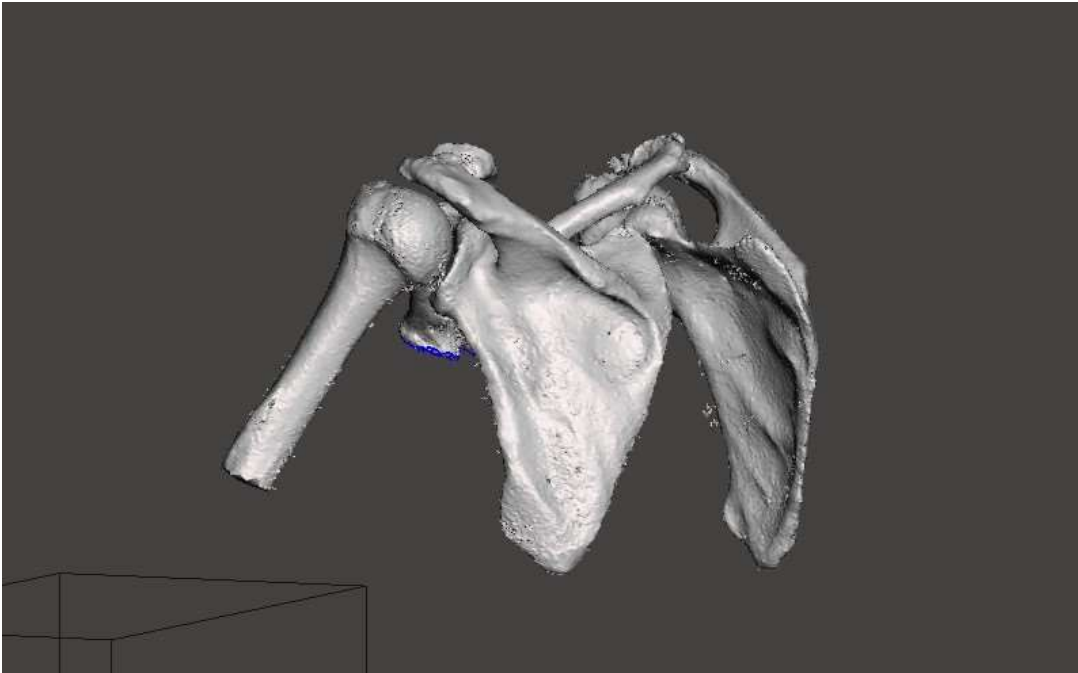


**Figure 9.** End product in Meshmixer.

The process of isolating the joints occupied an equally significant timeframe as creating the SRs, with the most common time frame (from importing to saving a copy) was an hour and a half. A word of caution: This process is prone to a myriad of issues if the proper choice of computer/external device is avoided for inferior technology.

Meshmixer requires a computer of ‘at least 32 GB’ according to the website manual; this is an erroneous suggestion, through experience with a 16, 32, and 64 GB (both Mac and Windows) laptop computers; 32GB is not sufficient to run a sample size higher than 50 with CT scans as detailed as the ones acquired from NMDID (scan field of views in a range of 350-699 mm). Alternate ID codes have been assigned to each individual for the purpose of random analysis. These codes were originally chosen via a digital randomizer set from 1-300 (no duplicates); however, this was changed when the total sample size

was cut in half (without revising any of the previous numbers) to 1-160 (still no duplicates) using the same digital randomizer. Often, time constraints required that both the Meshmixer stage and the OSIRIX MD stage occur concurrently through the use of two laptops and three external hard drives (really two when the very first one became corrupted).

### **Extra Guidelines and Materials Used**

For the purposes of this study, the decedent's vertebrae will not be assessed for OA. While it is true that the articular surfaces are also synovial joints, they are too small, too many, and too variable to be used in this study. The NMDID was used to acquire each complete individual's CT scans and metadata. The scans of each individual were uploaded onto OSIRIX MD and then converted to standard triangle language (STL) files. An STL file is a file type that uses a series of triangles to represent the surfaces of a solid model and is also regarded as the gold standard of data transfer from computer-aided design (CAD) software to 3D printers (Paramasivam et al., 2020). This conversion process is necessary to allow the CT scan to be opened as a 3D model. After the file is converted, it is opened in Meshmixer to be further refined before ultimately being scored. By refined, it is meant as the process used to isolate the intended joints and remove other shapes from the file.

A Macintosh (Mac Book Pro) computer laptop (with 36GB processing power) and Windows 11 version 23H2 run (MSI GE63 Raider) computer laptop (with a modified 64GB processing power) were used to conduct the image processing stage of this project. Generally, two computers became necessary during the data collection phase due to the

limitations of both OSIRIX MD and Meshmixer. A total of three five-terabyte (5TB) hard drives were used to store the CT scans and the 3D models. Once data collection was complete, the information was organized and processed in Excel before the construction of a mathematical model in SPSS. In this chapter, the methods used during the data collection phase are discussed along with vocabulary specific to those methods. During this chapter, the organization and quantification of the data collected are also briefly discussed.

### **Volume v. Surface Render**

One fundamental concept of 3D image analysis is the difference between a volume render and a surface render of CT scans. A volume render focuses on the data associated with human tissue and displays it; A surface render focuses on CT data to display the surfaces of the isolated segment (Udupa et al. 1991). Both render types create CT images that can be re-created from the same CT data. While a volume render would produce more images of visual depth, see **Figure 10** for an example of VR, it would only be a 2D image where no measurements or separation could take place.

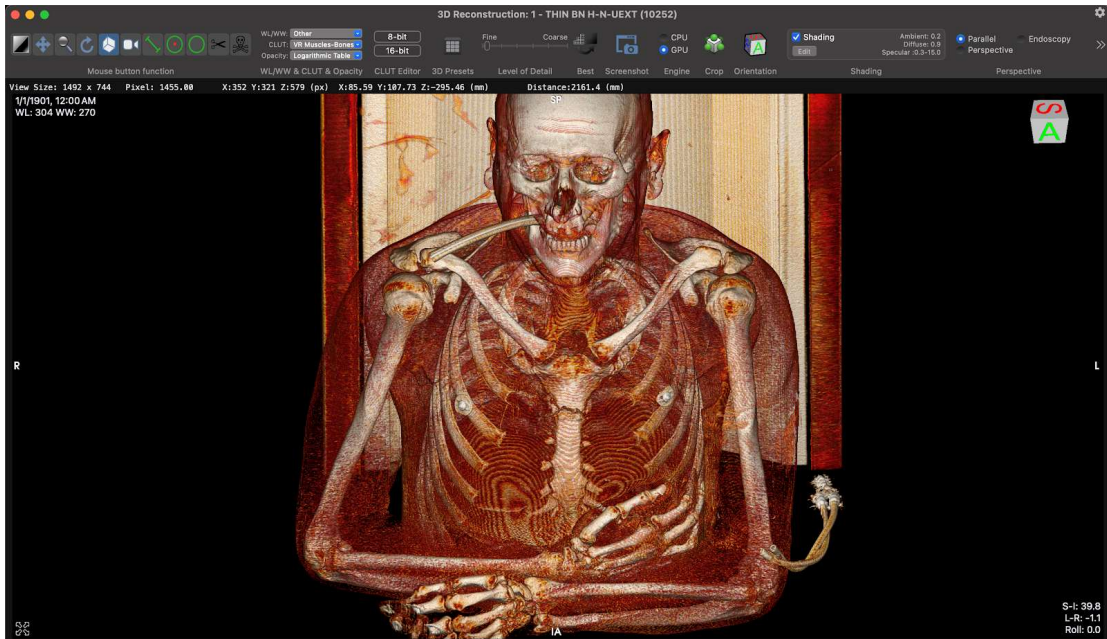


**Figure 10.** VR example in OSIRIX MD.

With a surface render, the 2D CT scan is converted into a stereolithographic format or standard triangle language (STL), which forms a 3D model that can be isolated and measured; in OSIRIX MD volume renders cannot be converted into STL files. Essentially, the volume render is a 3D image compared to the surface render's 3D printable model. A volume render generates a 3D image using all of the image slices from a CT scan to create a clear image, while the surface render only uses the slices required to generate a silhouette of the CT image (Rahim et al., 2017). Both 3D render types are usable in different academic or medical settings; however, only surface renders were generated for this project's purposes.

### Scoring Cleaned Scans

Since the images have received alternate ID codes, starting from ID1 and moving through the numbers, each joint was observed and scored following Jurmain (1990), as used in Winburn and Stock's (2019) study. This system looks at the degree of OA through the severity of joint change by assigning each joint a score from 0-3 based on visual assessment. A score of zero indicates little to no OA present on the joint; a score of 1 is indicated by evidence of small osteophyte presence and/or pitting of the articular surface over less than 10% of the overall surface; a joint score of 2 is indicated by a very large osteophyte remodeled and concave with original surface and or pitting more than 10% of the articular surface or presence of eburnation at any stage; and a score of 3 is indicated by ankylosis of the joint (Jurmain, 1990). In cases without OA, this method cannot be used to assess for age as this method requires at least an early form of OA to be present on the joint (Winburn and Stock, 2019). Sided combined joint scores for each joint (both left and right sides) were also calculated at this stage. This was done by adding and dividing the individual scores by the number of available elements. For example, the sided combined joint score for the right knee is equal to the right distal femur score plus the right proximal tibia score plus the right patella score, all divided by 3. Blended combined joint scores were also calculated by applying the sided combined joint score formula to the scores on both the left and the right side of a single joint. For example, the combined joint score for the knee is equal to the left distal femur plus the right distal femur plus the left patella plus the right patella plus the proximal tibia plus the distal tibia, all divided by 6. These scores were dichotomized into one of two categories,

OA present or OA absent, where OA present was any indication of OA (combined scores equaled to more than 0) and absent was no OA detected at all (combined scores equal 0). Presence or absence was noted along with each score with the intention of analyzing data with both the presence of OA as well as severity. In order to estimate age, the 95% age at transition from Winburn and Stock (2019) figure 9 (see **Figure 11**) is used for the oldest option where OA is present in a given individual. This was the standard used in cases where OA was present in only one joint and multiple joints (in the case of multiple joints, the oldest option was taken as the age estimate).

**TABLE 9** Ages of transition (mode) and ages at which 90% and 95% of European-Americans transition from "no osteoarthritis (OA)" to "OA present"—Defined here as any articular surface exhibiting any skeletal evidence of OA, however slight

Joint	Females			Males			Combined-sex		
	Mode	90%	95%	Mode	90%	95%	Mode	90%	95%
TMJ	23.2	77.3	93.6	NA—Do not use male TMJ			NA—Do not use TMJ		
Shoulder	19.5	42.3	47.8	24.0	40.1	43.5	22.2	41.6	45.9
Elbow <sup>a</sup>	14.2	45.8	55.2	18.0	33.1	36.5	12.4	39.2	47.0
Wrist	10.1	53.4	69.6	11.6	43.9	54.4	10.0	48.4	62.2
Hand	23.6	57.6	66.4	20.0	55.3	65.0	21.2	56.5	66.0
Hip <sup>a</sup>	13.0	37.2	44.0	16.4	29.7	32.7	11.7	32.7	38.6
Knee	0.3	27.3	55.1	11.4	41.3	50.7	6.1	40.6	54.8
	Use female knee only if necessary <sup>b</sup>						Use combined-sex knee only if necessary <sup>b</sup>		
Ankle	NA—Do not use female ankle			13.1	55.1	69.2	NA—Do not use ankle		
Foot	2.9	59.6	96.6	2.9	49.8	62.6	2.9	54.5	74.3
	Use female, male, and combined-sex foot models only if necessary <sup>b</sup>								

Notes: Absence of OA should only be considered conclusive in complete skeletal cases. In cases of fragmentary remains, only presence of OA can be used to inform an age estimate (i.e., "absence of evidence is not evidence of absence"). All ages are in years. Female, male, and combined-sex models are presented; sex-specific models should be used wherever possible.

Abbreviation: TMJ, temporomandibular joint.

<sup>a</sup>Small sample size for "no OA" (see Appendix S1).

<sup>b</sup>Low modes reflect extreme overlap in ages of individuals with "no OA" and "OA present." While several other models produced modal ages of transition younger than the youngest age in sample (i.e., elbow, wrist, hip, and male ankle models), the severity of this tendency in the female and combined-sex knee models and all foot models indicate that these models should be used with caution.

**Figure 11.** Table 9 from Winburn and Stock (2019).

### **Statistical Analysis**

For the analysis of the current study's results, the left and right joints were assessed both separately in Excel and combined in the Statistical Package for the Social Sciences (SPSS). Linear regressions were done on the individual joint scores to indicate an association between OA and age. What constitutes an individual joint score will be explained further in the next chapter, but to summarize it is the individual score for each bone in a joint. Intra-observer error was tested using the first seven individuals scored in the form of a Cohen Kappa test. The demographics of the intraobserver sample are as follows: 4 AFAB and 3 AMAB aged 37, 49, 55, 56, 61, 63, and 65. Further testing was done to illustrate how well the Winburn and Stock (2019) method performed over this study's sample. This included comparing the predicted ages with the recorded age at death in order to calculate the accuracy of Winburn and Stock's (2019) method on the current sample size. The Winburn and Stock (2019) comparison was conducted using blended combined joint scores for each individual. The numerical results and further details about how each test was run will be explained in the next chapter.

## RESULTS

Where the previous chapter discussed the methods employed in this project, this chapter presents the results of this project, as well as the statistical means by which they were achieved.). Of the total 150 individuals that make up the current study's sample size, only 85 displayed OA (present to some capacity) and thus only 85 individuals were candidates to have a predicted age using the Winburn and Stock (2019) method. SPSS is a software used for statistical analysis and data management (Obertova, Stewart, and Cattaneo, 2020). SPSS has a precedent for use in forensic analysis and other natural or health sciences due to its user-friendly interface and processing capabilities (Obertova, Stewart, and Cattaneo, 2020). Microsoft Excel was used to create scatter plots for separate joint analyses, which helped visualize trends within the data. Microsoft Excel was also used to organize and test various formulae on the project data to calculate averages, which gave a representation of how accurate the models were. The first section discusses the analyses conducted on the total population comprehensively (regardless of category). The following sections detail the results of analyses where the decedents are organized by age and assigned sex, as well as an analysis where the right and the left joints are assessed separately. Also explored in this chapter is how the current results compare to the suggested ages presented by Winburn and Stock (2019).

### Comprehensive Sample Analysis

A data sheet consisting of each joint examined was used to build a model to assess for age based on their individual joint scores. A numerical report of the number of joints scored is represented by **Table 2**.

Joints examined	Total # of joints	Bones in joint	Total # of bones
Shoulders (SH)	143	Prox. humerus, glenoid fossa (scapula)	286
Elbows (EL)	117	Dist. humerus, Prox. radius, and prox. ulna	351
Wrists (WR)	98	Dist. radius, dist. Ulna, lunate, scaphoid	392
Hips (HIP)	140	Acetabulum, prox. femur	280
Knees (KN)	126	Dist. femur, prox. Tibia, patella	378
Ankles (ANK)	132	Dist. tibia, dist. Fibula, talus	396

**Table 2.** All examined joints and bones.

Using SPSS, a linear regression model was conducted several times to fine-tune and test the accuracy of the model. The first output was sent through the regression linear function with the dependent variable set as age, and the independent variables were set as the combined scores of each joint, results shown in **Figure 12**. The second output kept age as the dependent variable and set the independent variable as all of the individual joint scores, results shown in **Figure 13**. Output 3 was created using select individual joint scores for the independent variable, as only those whose Output 2 significance level reading was less than 0.2, results shown in **Figure 14**. The elements retained for output 3 (significance values less than 0.20) were the scores for the right proximal humerus (RPH), left distal radius (LDR), left scaphoid (LS), left proximal femur (LPF), left

acetabulum (LA), right distal femur (RDF), and the right patella (RP). Output 4 chose 80% of the decedents using the same variables from output 3 and ran a linear regression with age as the dependent variable, results shown in **Figure 15**.

**Coefficients<sup>a</sup>**

Model		Unstandardized Coefficients		Standardized Coefficients	t	Sig.
		B	Std. Error	Beta		
1	(Constant)	37.922	2.893		13.107	<.001
	RSHComScor	-4.830	8.987	-.147	-.537	.593
	LSHComScor	3.293	8.650	.100	.381	.705
	RELComScor	-4.310	7.423	-.148	-.581	.564
	LELComScor	-.864	7.449	-.028	-.116	.908
	RWRComScor	38.052	30.470	.961	1.249	.217
	LWPComScor	-26.722	30.089	-.673	-.888	.378
	RHIPComScor	-12.765	15.293	-.488	-.835	.407
	LHIPComScor	24.088	16.100	.877	1.496	.140
	RKNComScor	-16.118	14.421	-.650	-1.118	.268
	LKNComScor	25.561	15.093	1.000	1.694	.096
	RANKComScor	38.720	35.382	1.215	1.094	.278
	LANKComScor	-37.364	35.531	-1.163	-1.052	.297

a. Dependent Variable: AGE

**Figure 12.** SPSS results of Output 1. Left and Right combined joint scores.

**Coefficients<sup>a</sup>**

Model		Unstandardized Coefficients		Standardized Coefficients	t	Sig.
		B	Std. Error	Beta		
1	(Constant)	37.870	2.889		13.107	<.001
	RProxHum	-15.699	8.580	-.491	-1.830	.073
	RScap	1.044	11.478	.033	.091	.928
	LScap	6.360	8.390	.199	.758	.452
	RDistHum	13.141	21.327	.458	.616	.541
	LDistHum	-11.377	24.762	-.371	-.459	.648
	RProxRad	-16.245	29.459	-.549	-.551	.584
	LProxRad	15.644	31.665	.528	.494	.623
	LDistRad	-15.231	8.926	-.438	-1.706	.094
	RDistUI	22.662	18.376	.604	1.233	.223
	LDistUI	-10.350	18.005	-.278	-.575	.568
	LScaph	11.883	7.280	.305	1.632	.109
	LProxFem	-10.245	6.333	-.391	-1.618	.112
	RAcet	-7.497	10.937	-.297	-.685	.496
	LAcet	32.471	13.384	1.208	2.426	.019
	RDistFem	-24.384	12.995	-1.056	-1.876	.067
	LDistFem	18.998	17.966	.784	1.057	.295
	RPatella	37.405	21.901	1.464	1.708	.094
	LPatella	-25.424	24.585	-.974	-1.034	.306
	LProxTib	2.451	13.776	.101	.178	.860
LDistTib	-5.844	9.513	-.195	-.614	.542	
LDistFib	-5.094	10.899	-.165	-.467	.642	
RTal	17.857	15.240	.578	1.172	.247	
LTal	-3.897	16.720	-.122	-.233	.817	

a. Dependent Variable: AGE

**Figure 13.** SPSS results of Output 2. Left and Right individual joint scores.

**Coefficients<sup>a</sup>**

Model		Unstandardized Coefficients		Standardized Coefficients	t	Sig.
		B	Std. Error	Beta		
1	(Constant)	39.039	2.420		16.134	<.001
	RProxHum	-3.964	3.587	-.123	-1.105	.273
	LDistRad	-8.449	5.122	-.252	-1.650	.104
	LScaph	14.840	5.409	.407	2.743	.008
	LProxFem	-6.462	4.081	-.245	-1.584	.118
	LAcet	18.247	4.274	.680	4.269	<.001
	RDistFem	-2.356	4.429	-.101	-.532	.596
	RPatella	12.162	4.976	.474	2.444	.017

a. Dependent Variable: AGE

**Figure 14.** SPSS Output 3 results. Output 2 Sig. <0.2.

**Coefficients<sup>a</sup>**

Model		Unstandardized Coefficients		Standardized Coefficients	t	Sig.
		B	Std. Error	Beta		
1	(Constant)	39.598	2.676		14.798	<.001
	RProxHum	-3.085	4.063	-.094	-.759	.451
	LDistRad	-8.636	5.578	-.265	-1.548	.127
	LScaph	13.580	5.863	.382	2.316	.024
	LProxFem	-6.662	4.395	-.252	-1.516	.135
	LAcet	18.874	4.747	.713	3.976	<.001
	RDistFem	-3.041	4.620	-.131	-.658	.513
	RPatella	12.018	5.105	.467	2.354	.022

a. Dependent Variable: AGE

**Figure 15.** SPSS Output 4 results. 80% participants with same Constants as output 3.

A model formula created from the constant variable b number of each variable whose significance value was 0.20 or lower reads as follows:

$$\text{AGE} = (-3.085 * \text{RPH}) + (-8.636 * \text{LDR}) + (13.58 * \text{LS}) + (-6.662 * \text{LPF}) + (18.874 * \text{LA}) + (-3.041 * \text{RDF}) + (12.018 * \text{RP}).$$

This formula was used to predict age against the total sample size (n=150) divided into 80% and 20% of participants. The formula was run on the data, and then the absolute value of those results was calculated and averaged. When the formula is used on 80% of the total sample size (n=120), the results indicate an age estimation within 12 years of accuracy. The same formula was then used on the remaining 20% (n=30), which yielded similar results of age estimation within 14 years of accuracy. This formula showed a tendency to under-age the individual more on than to over-age the individual, as in 84 of 85 individuals were underaged (-10 years) for this formula set, and no individuals were over-aged.

Further analysis of the current data was conducted using the combined joint scores derived from the individual scores used in the previous analysis. Combined joint scores were calculated following Winburn and Stock (2019), which is the summation of each individual joint score divided by the total number of elements in a joint. For example, the combined joint score of the left knee is equal to the scores for the left distal femur, patella, and proximal tibia divided by 3. To achieve a blended left and right combined joint score, this formula was applied across the data for the left and right of a single joint. For example, the blended combined joint score of an individual's knee is equal to the scores for the left and right distal femora, patellae, and proximal tibiae divided by 6. This was conducted with the aim of quantifying the presence or absence of OA in an individual. The model developed by Winburn and Stock (2019) was an "age at

transition” model that reflects the earliest age OA appeared in their sample and the average age at which OA was noted present for each joint type. The female knee and the combined knee limits were cautioned by Winburn and Stock (2019) to only be used if necessary. When applying the current results to Table 9 of Winburn and Stock (2019), only the comparable joints were examined (i.e. the ankle was left out of this analysis, but the knee was kept in as it was present, and the linear regressions suggested its value in this participant group). **Table 3** shows the numerical assessment of all joints that had OA present, and thus could be used to estimate age.

Joints examined	Total # of joints	Bones in joint	Total # of bones
Shoulders (SH)	66	Prox. Humerus, glenoid fossa (scapula)	132
Elbows (EL)	66	Dist. Humerus, Prox. radius, and prox. ulna	198
Wrists (WR)	43	Dist. radius, dist. Ulna, lunate, scaphoid	172
Hips (HIP)	90	Acetabulum, prox. femur	180
Knees (KN)	75	Dist. femur, prox. Tibia, patella	225
Ankles (ANK)	79	Dist. tibia, dist. Fibula, talus	237

**Table 3.** All joints and bones with OA present.

Overall, the predicted age results of the combined-sex model were more favorable when the predicted age was assessed within 20 years instead of 10 years; having a 64.28% and 41.07% age estimation accuracy percentage, respectively. Since the Winburn and Stock (2019) method was the only one used to estimate age, the results of age estimation accuracy within one year were also calculated and were found to have a 9.82%

accuracy; which was expected as no current method boasts a single year age estimation, this was done to be more concurrent with the age options as they are presented in Winburn and Stock (2019). The overwhelming trend was to underage the sample (82 out of 112 people underaged 11 to 67 years), although a few were overaged (21 out of 112 people overaged 11 to 36 years).

### **Sex Group Results**

The decedents were organized into AMAB (n=73) and AFAB (n=77) groups for further analysis. Both datasets' individual joint scores were run in SPSS for a linear regression analysis to determine which elements appear to have more influence in age estimation. The AFAB group had elements with a significance value of 0.09 or less in elements from the knees and wrists exclusively. The AMAB group showed elements with a significance value of 0.09 or less in elements from the hips, knees, and wrists, with the majority favored in the wrists. The linear models were inaccurate to age by a significant margin when tested; 33 to 42 years off with a tendency to under-age in the AFAB group and 31 to 41 years off in the AMAB group. There was little difference between the assigned sex groups when assessing broad trends; however, there was a significant difference from the comprehensive results (it appears inaccuracy increased when the sample was separated by assigned sex).

Winburn and Stock (2019), demonstrated a significant difference in the onset of OA between the assigned sex groups between the age of onset, age of transition, and which joints are more associated with age. While the current study's sample displayed

differences in accuracy, the assigned sex groups performed similarly to each other. Using OA presence to estimate age within 20 years, the AFAB group was found to have 75% accuracy, and the AMAB group had 68.75%. When examining the same data but within 10 years, the AFAB group was found to have 44.64% accuracy, and the AMAB group was found to have 37.5% accuracy to reported age at death. Only one person was aged accurately within 1 year in the AFAB group, and 9 people were accurately aged to 1 year in the AMAB group. Of the 56 AFAB individuals with OA present, 12 were overaged (anywhere from 11 to 40 years over), and 19 people were underaged (anywhere from 11-60 years). Of the 64 AMAB individuals with OA present, 14 were underaged (12-47 years), and 26 were overaged (11-40 years).

### **Age Group Results**

The decedents were organized into 10-year age groups for further analysis; this yielded seven groups ranging from 20 years old to 88. The groups consist of 20-29, 30-39, 40-49, 50-59, 60-69, 70-79, and 80+. The average group size was 21 decedents, although the range of group size was 19 to 25 decedents for a total of 150 individuals. There was some difference between the age groups where accuracy is concerned. The 20-29 age group was the most accurate, with the 40-49 age group performing nearly as well. The least accurate age group was the 80+ group. Only eight individuals across each category were over-aged no more than 5 years, the majority of which were found in the 30-39 age bracket. No individuals were over-aged in the 40-49, 70-79, or 80+ groups. Similar to the assigned sex groups, age predictability became less accurate for each group. When

accuracy is compared to the comprehensive results, the averages are in stark contrast by decades difference. Meaning here that when the linear regression results are compared to the comprehensive results, the difference in accuracy goes from about 14 years off to about 35 years off.

The full percentages of the age groups compared to Winburn and Stock (2019) can be seen in **Table 4**. In the 80+ group (n=19) all individuals presented with at least some OA, 21.05% were accurately aged within 20 years, and 15 people were underaged (19-46 years). No individual from the 80+ group was overaged, aged within 1 year, or aged within 10 years. For the 50-59 age group (n=26) all individuals with OA were accurately aged within 20 years, 78.26% were accurately aged within 10 years, 6 individuals were aged within 1 year, 4 had no OA present, 1 person was overaged by 12 years, and 4 people were underaged (anywhere from 11 to 19 years). In the 20-29 age group (n=21), 14 individuals had no OA, no individuals were underaged, and 7 were overaged (26 to 36 years). Also, within that age group, no individuals were aged accurately within 1 year, 10 years, or 20 years.

Age Group	Number of Decedents with OA Present	Within 20 years	Within 10 years	Within 1 year	Total overaged (10 year criteria)	Total underaged (10 year criteria)	Total number of Decedents
20-29	7	0	0	0	7	0	21
30-39	13	6	2	1	11	0	23
40-49	15	15	12	0	3	0	19
50-59	23	23	18	6	1	4	27

60-69	23	15	11	4	0	12	25
70-79	15	9	1	0	0	14	15
80+	19	4	0	0	0	19	19

**Table 4.** All age groups compared to Winburn and Stock (2019) results.

### Separate Joint Analysis

Separated left and right age assessments for each joint were conducted to assess for broad trends among the joints. For this analysis, scatter plots were made for each joint and each side to make visual observations of general trends. Each plot was assessed for a positive trend, indicating correlation, or a negative/scattered trend, indicating no correlation. On the left, several joints indicated a higher association with age than the others. The shoulder, the hip, and the knee displayed a higher association with age, and the elbow, wrist, and ankles showed a lesser association. On the right, an identical trend was observed for each joint, with only a few individuals making up the difference from the left counterpart. **Figures 16-17**, of the shoulders and ankles demonstrate a positive trend and a neutral trend.

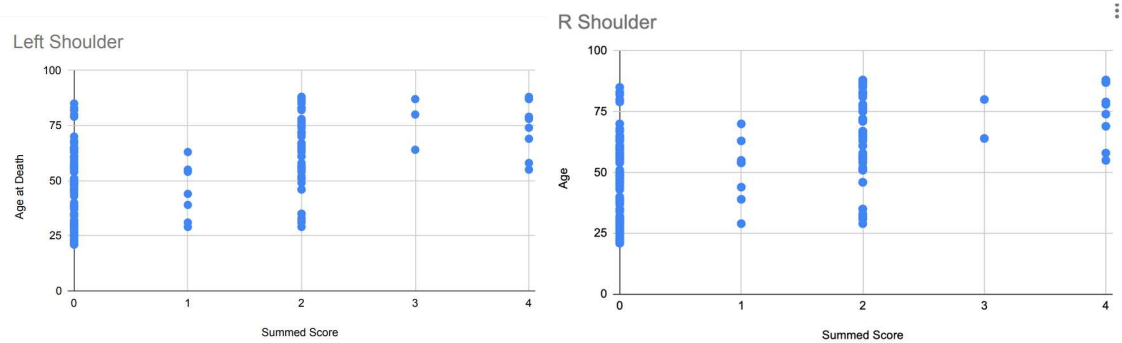


**Figure 16.** Left (left) and right (right) shoulder scatter plots. Positive trend example.

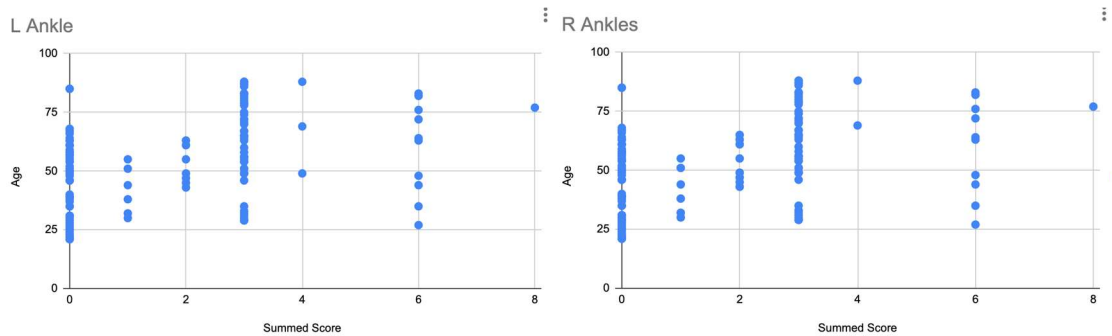


**Figure 17.** Left (left) and right (right) ankle scatter plots. Neutral trend example.

This is consistent with a similar assessment conducted by Winburn and Stock (2019), where the differences in right and left joint scores were not statistically significant enough to warrant separate analyses, which is why this author did not run formulaic statistics on each side as with the previous factors.

### Intraobserver Error Analysis

To assess for intraobserver error, a sample of the first seven individuals scored were chosen to be re-scored once a full 30 days had passed after the initial score was assigned.

For this analysis, the blended combined joint scores were tested against each other using a Cohens Kappa test in SPSS. See **Table 5** for a complete breakdown of the compared joints. Landis and Koch's (1977) degree of agreement was also used in the assessment of the intraobserver error.

Joints compared	n=	Approximate Significance	Landis and Koch Agreement
Shoulders	5	0.4	moderate
Elbows	2	N/A	N/A
Wrists	2	N/A	N/A
Hips	7	0.009	poor
Knees	6	<0.001	poor
Ankles	7	0.085	poor
Initial SH xHIP	5	0.8	good
Initial SH xKN	4	0.7	good
Initial SH xANK	5	0.6	good
Initial HIP xSH	5	0.6	good
Initial HIP xKN	6	1.00	very good
Initial HIP xANK	7	0.088	poor
Initial KN xSH	4	0.296	weak
Initial KN xHIP	6	0.845	very good
Initial KN xANK	6	0.184	poor
Initial ANK xSH	5	0.464	weak
Initial HIP	7	0.628	good
Initial KN	7	1.00	very good

**Table 5.** Cohen's Kappa results on intraobserver error.

The Landis and Koch (1977) scale is used to indicate relatedness of 0.8 to less than 0.02, where 0.8 indicates a strong connection and 0.02 indicates a very weak connection or agreement. All of the results presented in the current chapter will be explored further in the following chapter (Discussion Chapter).

## **DISCUSSION**

Where the previous chapter detailed the statistical results of the current project, this chapter will serve as a means to discuss those results. Moreover, this chapter covers a discussion of the immediate results of this paper, goes into the general themes and issues surrounding age estimation, technological tips learned through trial and error over the duration of the current study, ethically collected/ variety inclusion of human remains for study, and suggestions for future research based on current study limitations.

### **From The Results**

The results presented during the last chapter indicate an overall trend of somewhat accurately estimating the age of individuals between the ages of 40-70. When the age criteria from Winburn and Stock (2019) are used to estimate age, the minimum age possible to predict is 33.1 (male only), and the maximum possible age is 69.6 (female only). This range severely limits the possible age estimation, excluding the 20-29, 70-79, and 80+ age groups. In the context of how Winburn and Stock (2019) explain the method, in an ideal scenario, this method is not used in isolation, although it could be if the situation requires so. The age limitation of this method is a reminder that the 90% and 95% ages are meant to aid in narrowing an exhaustive predicted age range indicated by other aging methods, such as sternal rib end analysis or pubic symphysis examinations. As mentioned in the previous chapter, the predicted age results of the combined-sex model were more favorable when the predicted age was assessed within 20 years rather than 10 years and especially instead of just 1 year. If the situation requires the use of this

method singularly, then estimating age using the closest 20-year range, informed by the combined model's 95% age at transition, could provide more of an accurate age estimation than a 10 year estimate with the same information. The same can be applied to the sex-specific models as a similar pattern was observed: the amount estimated correctly within 20 years was reasonably higher than the 10 year estimate. Since only approximately 10% of the current sample study (who had OA present) was aged correctly within 1 year, the use of the Winburn and Stock (2019) method alone is not recommended for a digital sample; however, accuracy improves when attempting to estimate age within 10 years. This adheres to the field's standards as no method is accurate to a single year, results are often a range of several decades, hence the addition of the 20 and 10 year age buffer.

This method improves on several of the industry standards as it was able to achieve just over half the sample was correctly aged within 20 years and just under half correctly aged within 10 years. Some of the reasons the results turned out this way could be due to several factors that are outside the scope of this study to test. Human variation is notoriously complicated; even within a single population, the social lived experience of the decedents will be reflected in their osteological presentation (Ross and Pilloud, 2021). As previously stated, the current sample had individuals from the five major American-biased demographic ancestry groups, all of which had a unique social existence that likely impacted the severity and distribution of OA. This topic will be discussed further in this chapter as a suggestion for future research.

Within the assigned sex and age groups, the results show both broad similarities and glaring differences. To address the age groups first, there is a difference between the comprehensive joint scores and the individual element scores of each joint. The results from Winburn and Stock (2019) are somewhat consistent with the current study as the 90% and 95% ages from their age at the transition table are within the age groups whose accuracy performed comparatively better than other groups; the 40-49, 50-59, and 60-69 age groups. The age association linear regression test from the current sample indicates higher accuracy in the younger age groups (20-49), than the older age groups by a difference of 5 to 35 years. The 80+ group had the most inaccuracy overall, which could be attributed to the age limitation mentioned before, according to the method described by Winburn and Stock (2019). The comparison to Winburn and Stock (2019) continues this trend in the 80+ group, which had no accurately estimated individuals within 10 years or 1 year and only four individuals aged within 20 years. The same was observed in the 20-29 age group, and while the 40-49 and 70-79 groups had age estimations accurate to 10 years, there were no individuals accurately aged within 1 year. This overall trend is consistent with other aging methods in the field, which are often more accurate into the 30s and 40s but then become less specific as age increases into the older adult range (Albert & Maples, 1995; Hartnett, 2010; Webb & Suchey 1985). More on this trend will be explored in the following section.

The individual sex groups from the current study show little deviation from the combined joint score comparison. A considerable difference between AFAB, AMAB, and combined is that the AFAB group had more individuals aged correctly within 20

years (75% of those with OA present). This observation seems to be despite the female-only age estimation options (from Winburn and Stock (2019) Table 9) being limited to ages 44, 47.8, 55.1, 55.2, or 69.6. This limitation narrows the potential age pool noticeably. However, when estimating age within 10 years, the number of individuals who are aged correctly improves to 21 people out of the 57 who had OA present (44.64% of AFAB with OA), performing better than the AMAB group by little more than 6% and exceeding the combined group. The AFAB group also had fewer individuals with OA present (n=56 AFAB) than the AMAB group (n=64 AMAB). While the sex results are similar, they are not identical, which suggests sex-based skeletal differences (whether or not that's more due to lived experience rather than developmental biology is another question), a premise supported by results from Snodgrass (2004) as well as Winburn and Stock (2019).

In addition to the differences noted between sexes and age, there appears to be a slight difference between the left and right sides, which is consistent with the results discussed in Winburn and Stock (2019). The joints themselves are likewise not uniform in age association as the left and right shoulders, hips, and knees are the only joints to display a positive trend (indicating correlation) on their scatter plots. The joints not being equally associated with age is consistent with observations from Brenneman et al. (2016), who found the shoulder and the knee had the narrowest age margin of the joints assessed. Further assessment of joint age association within the current study support the observed trend, represented by the elements found to have a significance value of 0.09 or less. The joints included in this analysis include the wrist, shoulder, knee, and hip. The scatter plots

were a visual comparison of data, in contrast the linear regression used a formulaic approach to assess the data, which explains the apparent addition of the wrist between tests. The shoulders, wrists, and hips align with the results from Winburn and Stock (2019). However, in the current study, the knee was found to be a significant joint for estimating age in the combined group, specifically, the right distal femur and the right patella. The scatter plots and linear regressions from the previous chapter support some significance of the knee joint within the current study sample.

The intraobserver error noted in the previous chapter may have some bearing on how well the joints from this sample associate with age and the results from using Winburn and Stock's (2019) method. One reason for these results could be the visibility of each render. In multiple cases, it was difficult to differentiate between osteophyte activity and extra soft tissue being retained from the cleaning process (addressed later in this chapter as pill-bugging). This caused the observer to score more conservatively as the scoring progressed. The education and experience level of the observer likely also had some effect on the intraobserver results of this study, as experience remains the key determining factor in accuracy and speed of analyzing human remains (Spiros et al., 2023). Observer experience has been known to affect score reproducibility, with more experience leading to higher reproducibility on the same sample population (Langley et al., 2016). There was only a single person scoring whose field experience identifying and scoring OA is limited to a classroom setting, and who is educated to the degree of a Masters in forensic anthropology (by the completion of this thesis). Forensic anthropologists often have to rely on their expertise to conduct research; however, the

issue of education and conducting research on limited experience could be addressed with future research.

### **General Discussion**

As discussed in the previous research chapter, several other methods are used to examine OA as it relates to age-at-death. Strasheim et al. (2023)'s results demonstrated that the original methodology was accurate at estimating the age-at-death of BIPOC individuals. The findings from this study indicate the hip and shoulder were highly consistent and reliable during scoring and are thus recommended for use as the strongest indicators of age-at-death, while the TMJ and ankle performed poorly and should not be used for age estimation (Strasheim et al., 2023). Due to image visibility issues surrounding the TMJ on 3D renders, it was excluded from the current study. However, the indications of the hip, shoulder, and ankle are all consistent with the results observed in the current study. Strasheim et al. (2023) also reinforces the idea that a presence/absence methodology for OA-based age estimation is preferable to one based on the degree of severity when dealing with cases of fragmentary or incomplete remains, which is consistent with what Winburn and Stock (2019) reported; and what prompted the 80% joint visibility criteria for the current study.

Another method used to assess OA's use as an age indicator is Jurmain (1990) whose methodology shaped the criteria for scoring the Winburn and Stock (2019) sample, and thus the current sample. The results indicated significant differences between AFAB and AMAB joint scores, scores between joint types on the same individual, which side of the body the joint was on, and the level of disease progression in the joints

(Jurmain, 1990). While the current study is consistent with the difference between AFAB and AMAB scoring, there was no significant data to suggest a meaningful difference between OA progression on the left and right sides.

Brennaman et al. (2016) also explored the use of OA to estimate the age at death for individuals. The results of this study indicate this method of age estimation can be used only where all joint surfaces are complete, the left and right sides kept separate, and at least some OA is present; and becomes less precise threshold is in the 70+ range, which is an improvement on the previous 50+ range (Brennaman et al., 2016). The current study agrees that at least some OA needs to be present to use the method to estimate age and maintains that accuracy decreases past 70 years old. However, the current study indicates that accuracy among the younger adult ranges is not favorable, with a tendency to overage those in the 20-35 age range.

The results of Listi & Manhein (2012) conclude that vertebral OA alone is not enough information for accurate age estimation; also, the inconsistency of the intra- and interobserver changes could be due to the general definitions for each score, as terms such as “severe” and “slight” may not be detailed enough to assign a score. The verbiage issue is similar to what was presented in Fanton et al. (2010) and Hartnett (2010), with the descriptions of the auricular surface and sternal rib ends being influenced by interpretation (words like slightly, severe, or large are too vague to be used when describing physiological changes and impact repeatability). Winburn and Stock (2019) addressed this issue by providing a more detailed description of what constitutes a score for each joint.

The results from Snodgrass (2004) found only slight variation between the female and male groups used in the study, but the differences that are observed indicate osteophyte scores conducted in this manner have a higher accuracy for predicting age in males than females (Snodgrass, 2004). The conclusion from this result is that females show significantly greater variability in osteophyte stages which is not consistent with the observations of the current study. In the current study, the AFAB group was more accurately aged within 10 and 20 years than the AMAB counterpart. The Snodgrass (2004) conclusion may be relevant to how the current sample had less AFAB with OA present than AMAB as variability between a score of 0 and 1 would impact if an individual had OA present or not.

Much of the discussion around phase-dependent age estimation describes the physical appearance of each phase and how the changes in appearance associated to an age range (Albert and Maples, 1995; Fanton et al., 2010; İşcan et al., 1984; Webb and Suchey 1985). However, another issue that arises with methods dependent on one key factor is that they rarely take into account postmortem changes such as breakage (and subsequent bone loss) and other taphonomic changes. The taphonomic state of the decedent, while not a pathology, may also obscure an OA evaluation depending on the condition of the remains. Several factors can influence the preservation of bone from the moment of death; these include the physical properties of bone, decomposition, surrounding deposit environment, soil pH, predation, moisture content and oxygen levels (Pokines et al., 2022). Since taphonomy is an integral study when it comes to human remains, it bears repeating here that the previously discussed age estimation methods are

somewhat dependent on skeletal remains that have been preserved. While well-studied forensic anthropologists can distinguish postmortem skeletal changes from pathology, few studies attempt to cross study ideas of pathology and different taphonomic changes, due in part to the difficulty of determining what change was caused and when. This is an issue that can be addressed in further research.

### **Important Methodology Warnings**

Throughout the development of this project's methodology, I was struck with confronting some misconceptions about how setting up a digital analysis would be conducted. The process of reviewing the scans, obtaining the scans, rendering the scans, and finally analyzing the scans posed more challenges in practice than originally planned. This section aims to address some of the most glaring issues and offer ways to mitigate them for future study.

One must employ caution when selecting the sample from the NMDID, as the scout images are radiographs of each individual, not CT scans. There is no preview of the CT scan which accompanies the radiographs and the scout images are of a moderate quality. The difference in image types was mostly inconsequential as more often than not the issue of the decedent's personal effects obscuring relevant joints was more prevalent. Once the scans are processed through Meshmixer, most of the time, the personal effects can be removed, see **Figure 18**. However, this did create some 3D translations that could not be rendered properly due to metal objects interfering with the CT scan. This could have been avoided if the CT scans were conducted after the individual's personal effects

were removed. The table being visible is manageable; however, the inclusion of buttons, coins, bras, steel toe boots, jewelry, and other small personal objects are difficult to work around and are not required for skeletal analysis. Small intricate objects are arduous to remove without accidentally deleting the bones from the render. Likewise, large structures close to the body are difficult to remove without compromising the underlying structure

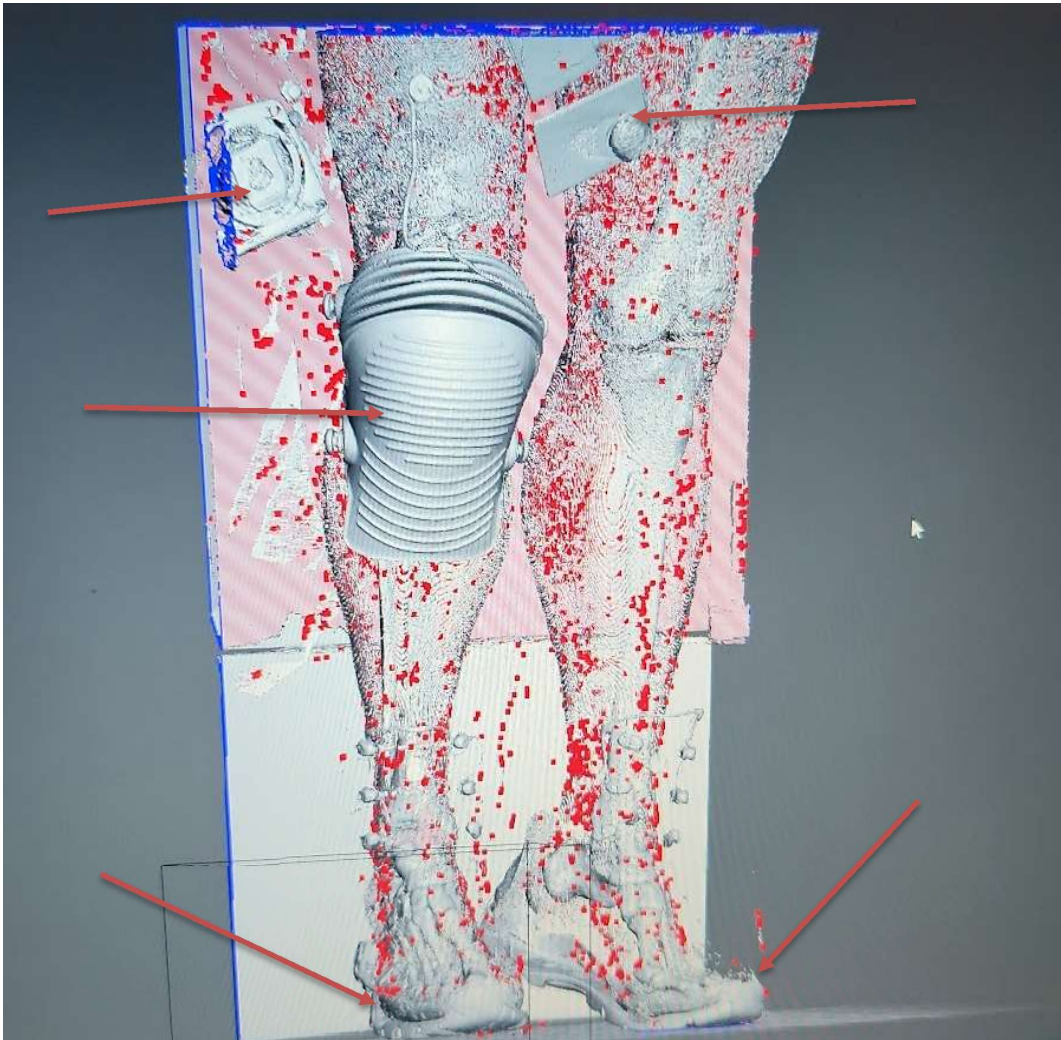


**Figure 18.** Personal effects on a 3D render. Within the image an apparent knee brace and other personal items (arrows) are present.

As of the time of writing, there is no acute way to automatically isolate bone material from non-bone material in Meshmixer (the materials must be highlighted individually for removal).

Importing and converting the CT scans through OSIRIX MD proved just as lengthy as the skeletal isolation process, partly due to the size and quality of the CT

scans. The NMDID uses scans that are 1mm thick with a 0.50 overlap (Vidoli, 2022). It is recommended to use a 1.25 mm maximum slice thickness when employing the use of 3D reconstruction in forensic casework (Ford and Decker, 2018). The extended time it took to open each file, render the images, open the images again and loading time during image cleanup is likely not due to the large file size of the CT scans and the capacity of both Meshmixer and OSIRIX MD. However, the CT density of each scan was not uniform, as is common since the CT density measures the density of tissues displayed on the CT scans (*embodi3D.com*, 2023). When using OSIRIX MD, the bone mean CT density is an important measurement and is used to isolate osteological material using the Region of Interest (ROI) tool (*embodi3D.com*, 2023). This function was intended to be implemented for the current study, but was unable due to the low density of several osteological structures; my experience indicates that the mean CT density needs to be over 1,000 in order to be selected manually. The inability to separate bone from the rest of the CT scan before converting the file into an STL is the likely cause of unusually bumpy areas of bone (e.g., pill-bug effect). This pill-bug effect was a major contender when assessing joint visibility as it was apparent that this phenomena was the result of the image rendering process, see **Figure 19**.

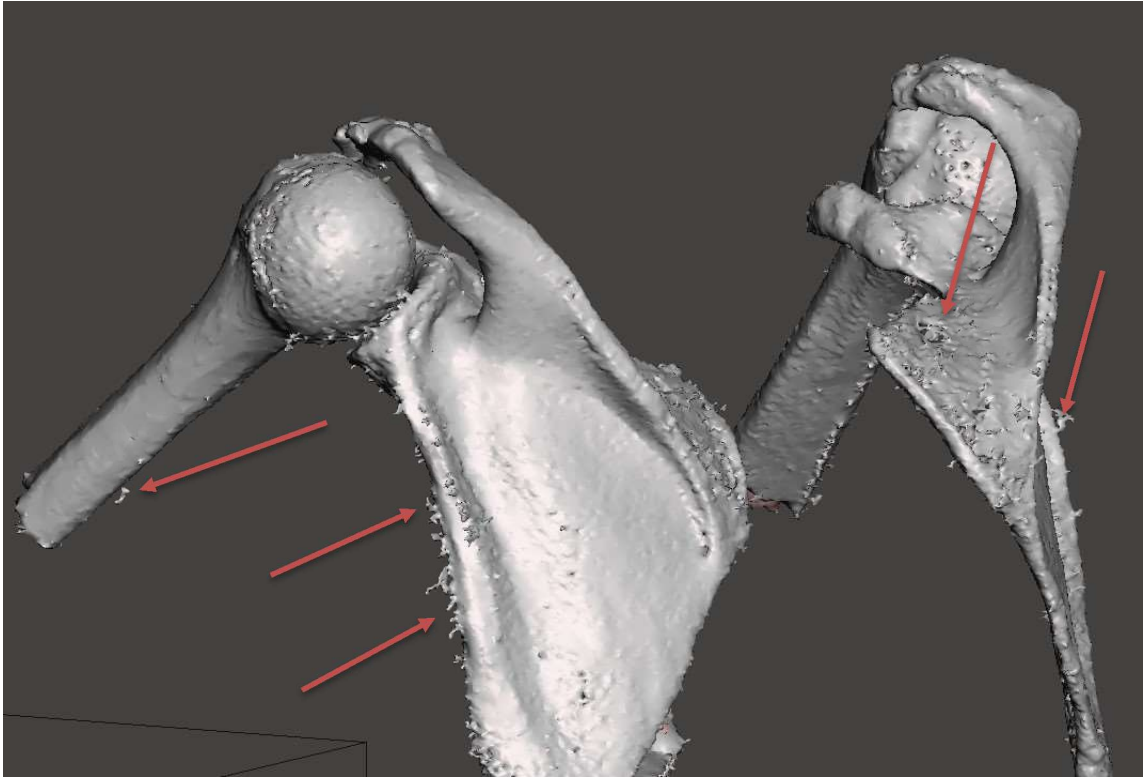


**Figure 19.** Pill-bugging. Extended surfaces rising off the rendered bone (arrows) caused by the rendering process.

The factor of the scan size and type may have impacted the overall results of the current study; however it appears that the CT density of the bone was the most influential in the issue of bone gapping, see **Figure 20**. Future research could be conducted testing the accuracy of differently sized CT scans for the purpose of examining skeletal remains.

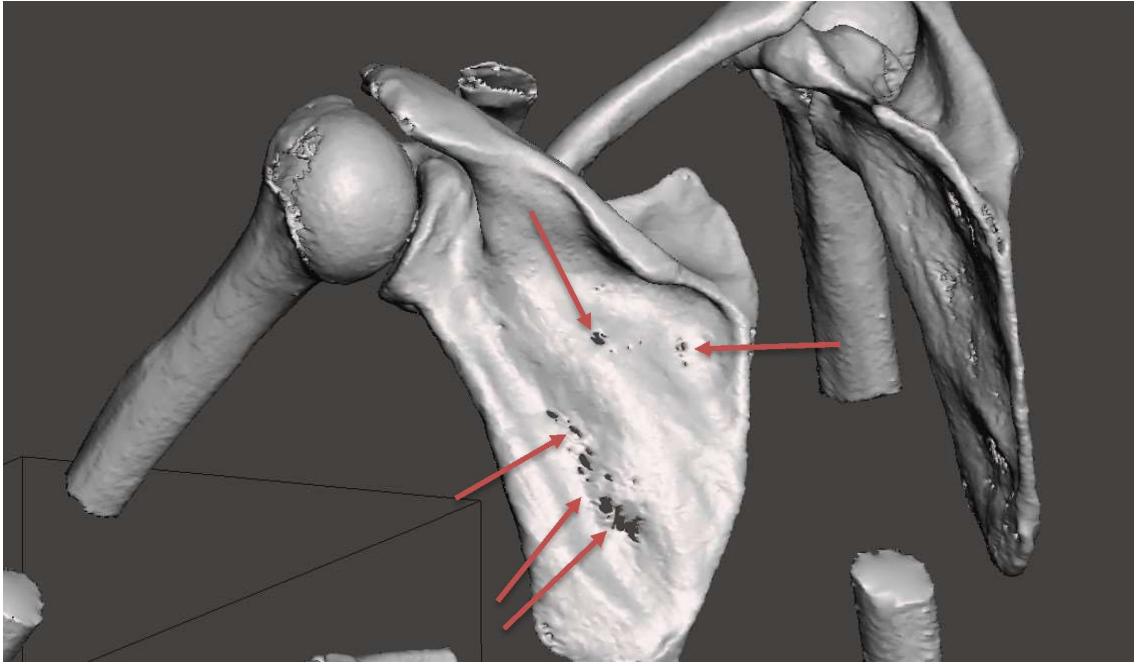


**Figure 20.** Cleaned 3D render. An example of bone gapping (arrows) where the thin surfaces could not fully render. Other common areas for this to occur is the cranium, distal femora, proximal tibiae, and iliac plate.

Another glaring misconception is that the manual of OSIRIX MD is sufficient to teach how to use the program. This was only partially false, as the manual does run through each function for its intended purpose; however, the instructions do not go into troubleshooting issues as they arise in practice. Turning to existing literature on the sole subject of using OSIRIX MD proved difficult; while previous researchers used OSIRIXMD for their projects successfully, they did not publish on the individual steps used to produce quality images (although they did present the end results and discuss what was done with the created images). It is my opinion that this publishing trend is due partly to publication requirements limiting what can be included in this final work. In which case only an effort to leave space for those steps or make available otherwise the

steps used when preparing 3D renders for analysis or printing. The other suspected factor as to why guided information is missing in the literature is due to the technical nature of including a step-by-step guide.

Through trial and error, means to remedy some of the processing issues encountered throughout this project include, at least a 32 GB with a 64GB preferred) and an external hard drive (this author recommends a 5TB SSD, possibly more than one depending on the scope of the project) to store the images on, are also required for this project. In addition, the requirements for using these media for conducting studies with a large sample size, and detailed imagery are not to be used on the minimum functioning requirements. A primary example of this is that while the OSIRIX MD minimum processing was stated as 16 GB of RAM, this processing power allows the program to do little more than open a CT scan file (of the caliber of the NMDID descendants) before struggling to open the same file as a surface rendering (SR), a process that took at minimum one hour per individual, often longer, and then further struggling to convert the SR into a .stl file. This was especially the case when decedents were mass pre-loaded into OSIRIX MD. One should only do 5 at a time and then delete once the files have been converted. Similarly, Meshmixer states its minimum to be 16GB of ram; however, this processing power often leads to the program closing itself while trying to open one .stl file. It should be noted that as of 2018, Meshmixer is no longer being updated, but is still functional, so these crashes will likely never be resolved (*Meshmixer*, n.d.). However, once the render is imported to Meshmixer and the file opens, which took an average of 30 minutes, but could take as long as 2 hours, lagging image positioning becomes an issue.

This issue has an easy fix as the more unwanted structures were removed from the scan, and the easier the image could be turned and modified.

The purpose of including this segment is to highlight the difficulties surrounding this project in the hopes of informing the next researcher who aims to study any of the related topics. This segment is in no way intended to state (implicitly or otherwise) that research involving digital remains or computer programming is not worth the endeavor. Several of the most time-consuming issues had relatively easy fixes (have a 64GB computer, use SSD external drives totaling 10TB, and remove large chunks of unwanted structures first and then get more detailed) that were eventually implemented during the course of this project. While, yes, several technological issues set the timeline of this project back, that a future researcher may not experience because of the inclusion of the imperfect improvising and pivoting required to complete the current study.

### **Avenues for Future Study**

Several suggestions for future research have already been mentioned in this chapter. This segment is meant to expand on some of them; however, any of the more casually mentioned avenues are still possibilities. To begin, a more detailed future study testing the Winburn and Stock (2019) method concurrent to other widely used age estimation methods, such as the Suchey-Brooks or sternal rib analysis, may provide insight on how to tune the accuracy of the method further. While the results of the current study support the use of the Winburn and Stock (2019) age-at-transition method, it was beyond the scope to test other aging methods directly with Winburn and Stock (2019).

This could look like combining estimates of another widely used age method and then using the results of Winburn and Stock (2019) to narrow large predicted age ranges, with the aim of seeing what methods provide more accurate results using Winburn and Stock (2019).

On the issue of a lack of specificity in older adult age ranges, it is a common theme for age estimation techniques (OA use or otherwise) for the predicted age ranges to be wide. A justification of wide age ranges is to accommodate for human variation between stages of skeletal change (Buckberry and Chamberlain, 2002). While the results of the current study only appear to reinforce this gap in age estimation, the potential for older age specificity is not lost entirely. The use of a broad age range, such as 50+, technically encompasses older age ranges; it does so without specificity (Baldsen et al. 2021). What's more is the use of sweeping older age ranges like those used in the Suchey-Brooks (1990) and İşcan et al. (1984) methods limit the specificity of older adult ranges (60s, 70s, and 80s). A path forward consists of conducting age-related studies with a specific focus on isolating older age identification means. Another option could be to re-examine current methods in the hopes of tailoring them for specificity among the older age ranges. For example, Hartnett's (2010) method, which was mentioned in the previous research chapter, added an additional 7th phase to allow anthropologists to place individuals into later morphological phases.

Future studies could test other forensic methods using 3D-rendered remains as the sample medium. This is not limited to using only SRs to study 3D-rendered remains but also VRs. An example is Alibrio and Tallman's (2024) research examining the effects of

cancer and cancer treatment on skeletal age estimation using CT 3D VRs. Among the positive aspects of having a sample consisting of only digital skeletal remains is the benefit of preserving the remains in the state they appeared when they were brought in to be scanned. They could be implemented in learning institutions so that students can learn in a classroom environment how to use these programs and benefit from exposure. Further studies could be conducted comparing the efficacy of SR and VR 3D models using landmarks commonly used to estimate age. A related avenue for future study could be to compare efficacy and ease of use on DICOM viewers so that we can start looking for a way to standardize their use. During the initial research for the current study, several programs (both free and monetized) were brought to the surface. To name a few, aside from Meshmixer and OSIRIX MD, there is RadiANT, Blender, OSIRIX LITE (the free version of OSIRIX MD), 3D slicer, and Materialize Interactive Medical Image Control System (also referred to as MIMICS).

Another topic of future research is to further expand age estimation methods to a population-based model or testing Winburn and Stock (2019) with a focus on population affinity like in Strasheim et al. (2023). As mentioned in the previous research chapter, Strasheim et al. (2023) conducted a validation study of Winburn and Stock (2019) by testing its accuracy on a BIPOC sample. When the white sample was compared to the BIPOC sample, the results were highly comparable, 88% and 85% respectively, when compared to the 95% age at transition (Strasheim et al., 2023). These results suggest that the Winburn and Stock (2019) method is applicable to a broad range of North American populations. However, the definition used for BIPOC grouped together individuals

belonging to multiple communities of color, an issue addressed in their study limitations (Strasheim et al., 2023). The demand for more population specific methods has been a common research idea for a while now. For example, a modern-age example of estimating the age of unknown individuals was conducted by Komar (2003), who utilized Bosnian mass graves to evaluate current practices in forensic anthropology and found that the most accurate age estimation methods are prevalent to young adults. The distribution of reported ages for the missing individuals in Bosnia in the early 2000s ranged from less than 10 years old to over 70 years old, with those in the study sample ranging from 16 to 71 years old (Komar, 2003). Within that sample those aged 30-50 represented most of the sample (43%), and the results found that 68.8% of the 16-30 year olds and 47.8% of the 30-50 year olds were correctly identified but only 20% of the 50+ group were correctly identified. However, in Komar (2003), one of the reasons attributed to the inaccuracies observed was the use of standards created using North American samples that had not been meaningfully tested on Eastern European populations. A focus on re-testing already existing methods should be conducted with the aim of testing accuracy among different populations (Ross and Pilloud, 2021). An example of this could also be re-framing categorical systems used in death investigations (such as the NMDID's) to follow a more population-oriented approach.

Another positive aspect of using digital forensic databases is the development of new forensic databases, which aids in limiting identification bias by allowing more inclusivity in study sample pools (Dirkmatt et al., 2018). Skeletal collections are used in the present day to study human remains and develop various analytical techniques;

however, diversity among the most used collections has been called into question in recent years (Strasheim et al, 2023). The term diversity in this context refers to a variety of any given human category (age, sex, and population affinity more so than stature). However, another limitation of skeletal collections is access, as nearly all of them reside in a single location and thus, anthropologists must have the means to travel to use the collection if they are not a part of the institution who hosts the collection. A common workaround for this and the issue of recreating damaging conditions to study effects on skeletal material is the use of nonhuman remains (Christensen and Smith, 2013). However, there are several limitations to using animal remains in forensic study since animal bones are a different structure and thus will behave differently when compared to human skeletal material (Christensen et al., 2022). Body and decomposition facilities have arisen as a means to study human remains ethically; however, morgues remain an underexplored avenue. This is largely due to restrictions concerning legal issues, decedent rights, and consent of the next of kin. It goes without saying, the moral and religious issues of individuals are inherently valid, and anthropologists have an obligation to respect religious/cultural practices surrounding death/mourning. One of the most admirable qualities of the NMDID is their standard for living relatives' consent and information documentation. With consent given from remaining relatives or as a specified method of donating your body to science, X-rays, and CT scans of decedents can be used to further the advancements of forensic study with real human subjects. Digital collections like the NMDID provide access for international study of regional-

specific remains, and provide a layer of consent for those related to the decedent for their loved one to be used in forensic study and teaching.

### **In Summation**

While much of this chapter has been about improvements that can be made with future study, this author does not want the main purpose of the current study to be lost. The results of the current research display promising numerical outputs and support the use of 3D-rendered CT scans (where traditionally there would be dry bone) as being comparable to results of other age estimation methods. While none of the categories (combined-sex, AFAB, and AMAB) agreement exceeded 50%, the current study was successful in accurately estimating age to roughly 40% of the sample with OA present within 10 years. When comparing age estimation accuracy within a 20-year span, the current study was accurately able to estimate age to 64% for the combined score, 75% for the AFAB group, and 69% for the AMAB group. Even though it was used in isolation, the method discussed in Winburn and Stock (2019) performed well when estimating the age at death of the current study's sample size.

## CONCLUSION

The difference between chronological age and skeletal age is an important distinction when it comes to discussing age estimation of skeletal remains (McCulloch et al., 2017). When forensic anthropologists estimate the age of skeletal remains, what is actually being estimated is the skeletal or developmental changes that occur as bone matures (Moorrees et al., 1963). The definition of age as it is examined in the current study is that of skeletal age at the time the individual died. OA was examined as means to estimate the age of 150 known decedents using 3D rendered models of their CT scans and methodology laid out by Winburn and Stock (2019). The results of this study predicted age was assessed accurately within 20 years for 64.28% of those with OA present and for 41.07% aged within 10 years.

Age estimation methods constitute a long and complicated list of techniques that can be used to approximate the age at death of an unknown individual. The various types of age estimation methods can be divided into two major groups, those that are more suited to juvenile age estimates and those that are suited to adult age estimates. The juvenile estimate methods include dental development, maxillary suture closure, and epiphyseal fusion of several bones (Albert & Maples, 1995; AlQahtani et al., 2010; Gruspier and Mullen, 1991; Mincer et al., 1993; Webb & Suchey, 1985). There is some overlap to the adult age ranges with several of the juvenile age estimation methods, so they may be used to exclude age groups; thus, they aid in determining which method may be more appropriate to use in a given case. The adult estimate methods include sternal rib analysis, pubic symphysis phase examination, iliac auricular surface examination, and

dental wear (Berg, 2008; Buckberry & Chamberlain, 2002; Hartnett, 2010; Katz & Suchey, 1986; Lovejoy, 1985; İşcan et al., 1984). In addition to examining the developmental changes of the skeleton, pathological changes can be used to approximate age. An example of this is the use of OA to estimate age due to its strong correlation to age (Alves-Cardoso & Assis, 2018; Brennaman et al., 2016; Listi & Manhein, 2012; Snodgrass, 2004; Winburn & Stock, 2019). The method posed by Winburn and Stock (2019) is useful for estimating age and should be explored further with new mediums and new collections. An example of this has already been conducted with the validation study by Streishem et al. (2023), where BIPOC population (albeit from the same collection) was examined using the same scoring method. Further research into other groups could include a study using Winburn and Stock (2019) to estimate age in non-American populations to see if the method can be applied more broadly.

There is no stand-alone method that estimates any one aspect of the biological profile; each parameter requires the implementation of multiple techniques and the combination of the results. The results of the current study suggest OA as a means to estimate age is no different from the established precedent of other age estimation techniques. OA is a multifactorial disease that has a richly explored connection to increased age. There are several factors that have been explored as influencing OA, but age of the individual has been the most consistent (Winburn and Stock, 2019). Other degenerative joint diseases may present similarly to OA, but with training and exposure, it may be possible to distinguish them from one another (Burt et al., 2013). The very nature of OA warrants further study as the cause of OA developing in a given joint is

only somewhat understood. OA is a disease that has several factors to influence the development and severity of the disease; these factors include but are not limited to BMI, occupation, age, and sex (Burt et al., 2013). Not all the synovial joints are equally prone to develop OA; the ankle and elbow joints are not commonly affected and when the elbow is it is most commonly affected in the radio-humeral joint (Waldron 2009). However, the results of the current study indicate a different pattern as several elbows where OA was present in the ulnar aspect of the joint were scored. Since there are several factors that contribute to the development of OA, an attempt should be made to identify and analyze them (Listi and Manhein, 2012; Winburn and Stock, 2019). Research in this area, focusing on the social factors surrounding disease as well as the biological factors, would provide a comprehensive approach to epidemiology by adding focus to the underlying societal factors that contribute to pathology (Wemrell et al. 2016).

The use of an all-digital sample to conduct forensic study opens the door for further research using virtual anthropology. What's more, the use of digital programs, such as OSIRIX MD and Meshmixer, in forensic study provides a view of the various ways these technologies can aid further understanding in the field. Virtual Anthropology has taken form in the last decade as a study pathway that aims to integrate anthropology and technology (Weber & Bookstein, 2017). The current study argues that the use of medical imaging in forensic study is reinforced by its previous use in analytical research (Alves-Cardoso & Assis, 2018; Franklin et al., 2016; Kurenov et al., 2015). One of the ways medical imaging can benefit forensic study is the creation of digital databases such as the NMDID. Implementing use of digital databases in cases where physical collections

may not be possible would broaden the theoretical landscape by providing increased access to remains for study. The current study is not advocating for the replacement of traditional human skeletal collections, but rather to make common collections that are more accessible through digital media.

Through the use of OSIRIX MD and Meshmixer, in lieu of physical elements, OA was explored yet again as a means to estimate age. The method detailed by Winburn and Stock (2019) is a valuable resource when trying to narrow a sweeping age range, as their 95% estimate age for OA presence (combined-sex model) was able to accurately age nearly half the current study within 10 years. Despite several technological learning curves that needed to be overcome during the course of this project, the use of these programs was accurate in representing a skeletal sample. The capacity of OSIRIX MD and Meshmixer can be improved when using high-capacity computers. In the previous chapter, this author mentioned how there appears to be a lack of detailed explanations when it comes to publications using OSIRIX MD and Meshmixer. To avoid this in the future, publications that utilize either of these programs ought to prioritize detailed explanations of program methodology (and not just hide quick tips in figures). Or otherwise make available the information alongside the article (via program files or in with datasheets).

There are two major topics addressed in this project. The first is the use of an all-digital sample, and the second is exploring OA as an age estimation method. While there are things that cannot be learned from an all-digital collection (taphonomic color changes, texture changes, the feeling of hollow bones etc.), there is merit in having

accessible remains where research can be done to further our understanding of the field. When using digital material in the future, part of the goal should be to build literature not just of how they can be used but how they are being used. OA and other degenerative joint diseases are observed in modern humans, historic humans, and non-human animal groups; as such, studies with any of the sample groups furthers a holistic understanding of the causes behind OA development. While none of the methods or results turned out perfect, the potential for further research on both the use of OA as an aging method and the use of 3D-rendered bones for analysis is enough for this author to say this was productive.

To culminate this document, a reminder: The work we do is important. Age estimations for unknown individuals are still important for forensic investigators as an estimate of 46,709 cases of homicide and non-negligent manslaughter went unsolved from 2017 to 2022 according to the FBI's Uniform Crime Report data, and any new information can spark a lead (*Cold case homicide stats - project: Cold case*, 2024). There is the potential to expand on all of the topics mentioned in this document, but especially the concept of digital bone analysis and OA as a means to estimate age.

## BIBLIOGRAPHY

- Adams, D. C., & Otárola-Castillo, E. (2013). geomorph: an R package for the collection and analysis of geometric morphometric shape data. *Methods in Ecology and Evolution*, 4(4), 393–399. <https://doi.org/10.1111/2041-210x.12035>
- Adejuyigbe, B., Kallini, J., Chiou, D., & Kallini, J. R. (2023). Osteoporosis: Molecular pathology, diagnostics, and therapeutics. *International Journal of Molecular Sciences*, 24(19), 1–18. <https://doi.org/10.3390/ijms241914583>
- Albert, A. M. and W. R. Maples (1995) Stages of epiphyseal union for thoracic and lumbar vertebral centra as a method of age determination for teenage and young adult skeletons. *Journal of Forensic Sciences* 40(4):623–633.
- Alibrio, M. N., & Tallman, S. D. (2024). The effect of cancer and cancer treatment on pubic symphysis age estimation using computed tomography scans. *Diagnostics*, 14(14), 1500. <https://doi.org/10.3390/diagnostics14141500>
- AlQahtani, S. J., Hector, M. P., & Liversidge, H. M. (2010). Brief communication: The London atlas of human tooth development and eruption. *American Journal of Physical Anthropology*, 142(3), 481–490. <https://doi.org/10.1002/ajpa.21258>
- Alves-Cardoso, F., & Assis, S. (2018). Can osteophytes be used as age at death estimators? Testing correlations in skeletonized human remains with known age-at-death. *Forensic Science International*, 288, 59–66. <https://doi.org/10.1016/j.forsciint.2018.04.034>
- Archer, C. W., Dowthwaite, G. P., & Francis-West, P. (2003). Development of synovial joints. *Birth Defects Research Part C: Embryo Today: Reviews*, 69(2), 144–155.
- Aufderheide, P., Rodríguez-Maffiote Martín, C., & Langsjoen, O. (1998). *The Cambridge Encyclopedia of human paleopathology*. University Press.
- Berg, G. E. (2008). Pubic bone age estimation in adult women. *Journal of Forensic Sciences*, 53(3), 569–577. <https://doi.org/10.1111/j.1556-4029.2008.00712.x>
- Berry, S. D., & Edgar, H. J. H. (2021). Announcement: The New Mexico Decedent Image Database. *Forensic Imaging*, 24, 200436. <https://doi.org/10.1016/j.fri.2021.200436>
- Boldsen, J. L., Milner, G. R., & Ousley, S. D. (2021). Paleodemography: From archaeology and skeletal age estimation to life in the past. *American Journal of Biological Anthropology*, 178(S74), 115–150. <https://doi.org/10.1002/ajpa.24462>
- Brennaman, A. L. (2014). *Examination of osteoarthritis for age-at-death estimation in a modern population* [Master's Thesis, Boston University] <https://open.bu.edu/handle/2144/13305>

- Brennaman, A. L., Love, K. R., Bethard, J. D., & Pokines, J. T. (2016). A Bayesian Approach to Age-at-Death Estimation from Osteoarthritis of the Shoulder in Modern North Americans. *Journal of Forensic Sciences*, 62(3), 573–584. <https://doi.org/10.1111/1556-4029.13327>
- Brooks, S., Suchey, J.M. (1990). Skeletal age determination based on the os pubis: A comparison of the Acsádi-Nemeskéri and Suchey-Brooks methods. *Human Evolution*, 5, 227–238. <https://doi.org/10.1007/BF02437238>
- Buckberry, J. L. and A. T. Chamberlain (2002) Age estimation from the auricular surface of the ilium: A revised method. *American Journal of Physical Anthropology* 119, 231–239.
- Buikstra JE, Ubelaker DH. (1994) Standards for data collection from human skeletal remains. Fayetteville, AR: Arkansas Archeological Survey Research, 1994; Series No. 44.
- Burt, N. M., Semple, D., Waterhouse, K., & Lovell, N. C. (2013). *Identification and interpretation of joint disease in paleopathology and forensic anthropology*. Charles C. Thomas, Publisher, Ltd.
- Buser, T. J., Sidlauskas, B. L., & Summers, A. P. (2017). 2D or Not 2D? Testing the Utility of 2D Vs. 3D Landmark Data in Geometric Morphometrics of the Sculpin Subfamily Oligocottinae (Pisces; Cottoidea). *The Anatomical Record*, 301(5), 806–818. <https://doi.org/10.1002/ar.23752>
- Buzayan, M. M., Seong, L. G., Elkezza, A., Abdin, Z. B. Z., Yunus, N. B., & Sivakumar, I. (2020). Digital workflow for articulating maxillary and mandibular 3D arch models using an open source 3D modeling software program. *General Dentistry*, 51(9), 776–779.
- Christensen, A. M., Hefner, J. T., Smith, M. A., Isa, M. I., Berryman, H. E., & Web, J. B. (2022). Forensic Fractography of Bone: A New Approach to Skeletal Trauma Analysis. *Forensic Anthropology*, 1(1), 32–51. <https://doi.org/10.5744/fa.2018.0004>
- Christensen, A. M., & Smith, V. A. (2013). Rib butterfly fractures as a possible indicator of blast trauma. *Journal of Forensic Sciences*, 58(s1), S15–S19. <https://doi.org/10.1111/1556-4029.12019>
- Cold case homicide stats - project: Cold case*. Project. (2024, February 13). <https://projectcoldcase.org/cold-case-homicide-stats/>
- Dahaghin, S., Bierma-Zeinstra, S. M. A., Reijman, M., Pols, H. A. P., Hazes, J. M. W., & Koes, B. W. (2005). Does hand osteoarthritis predict future hip or knee osteoarthritis? *Arthritis & Rheumatism*, 52(11), 3520–3527. <https://doi.org/10.1002/art.21375>

- Dirkmaat, D. C., Cabo, L. L., Ousley, S. D., & Symes, S. A. (2008). New Perspectives in Forensic anthropology. *American Journal of Physical Anthropology*, 137(S47), 33–52. <https://doi.org/10.1002/ajpa.20948>
- Edgar, HJH; Daneshvari Berry, S; Moes, E; Adolphi, NL; Bridges, P; Nolte, KB (2020). New Mexico Decedent Image Database. Office of the Medical Investigator, University of New Mexico. [doi.org/10.25827/5s8c-n515](https://doi.org/10.25827/5s8c-n515).
- Ford, J. M., & Decker, S. J. (2018). Computed tomography slice thickness and its effects on three-dimensional reconstruction of anatomical structures. *Journal of Forensic Radiology and Imaging*, 4, 43–46. <https://doi.org/10.1016/j.jofri.2015.10.004>
- Franklin, D., Swift, L., & Flavel, A. (2016). ‘virtual anthropology’ and radiographic imaging in the Forensic Medical Sciences. *Egyptian Journal of Forensic Sciences*, 6(2), 31–43. <https://doi.org/10.1016/j.ejfs.2016.05.011>
- Fanton, F., M.-P. Gustin, U. Paultre, B. Schrag, and D. Malicier (2010) Critical study of observation of the sternal end of the right 4th rib. *Journal of Forensic Sciences* 55, 467–472.
- Fruciano, C. (2016). Measurement error in geometric morphometrics. *Development Genes and Evolution*, 226(3), 139–158. <https://doi.org/10.1007/s00427-016-0537-4>
- Gilmour, R. J., & Plomp, K. A. (2022). The changing shape of palaeopathology: The contribution of skeletal shape analyses to investigations of pathological conditions. *American Journal of Biological Anthropology*, 178(S74), 151–180. <https://doi.org/10.1002/ajpa.24475>
- Gruspier, K., & Mullen, G. (1991). Maxillary suture obliteration: A test of the Mann Method. *Journal of Forensic Sciences*, 36(2), 512–519. <https://doi.org/10.1520/jfs13052j>
- Guilak, F., Nims, R. J., Dicks, A., Wu, C.-L., & Meulenbelt, I. (2018). Osteoarthritis as a disease of the cartilage pericellular matrix. *Matrix Biology*, 71–72, 40–50. <https://doi.org/10.1016/j.matbio.2018.05.008>
- Hartnett, K. M. (2010) Analysis of age-at-death estimation using data from a new, modern autopsy sample—Part I: Pubic bone. *Journal of Forensic Sciences* 55(5), 1145–1151.
- How to create 3D printable models from medical scans in 30 minutes using free software: Osirix, Blender, and Meshmixer.* [embodi3D.com](https://www.embodi3d.com). (2023, May 18). <https://www.embodi3d.com/blogs/entry/193-how-to-create-3d-printable-models-from-medical-scans-in-30-minutes-using-free-software-osirix-blender-and-meshmixer/>

- Huffer, D. (2021). The osteology and provenance of a portion of the Parkinson collection, Gazelle Peninsula, New Britain, c. 1897. *International Journal of Osteoarchaeology*, 32(1), 156–169. <https://doi.org/10.1002/oa.3052>
- İşcan MY, Loth SR, Wright RK. (1984) Age estimation from the rib by phase analysis: white males. *Journal of Forensic Sciences*, 29(4), 1094–1104. PMID: 6502109.
- Jurmain, R. (1990). Paleoepidemiology of a Central California prehistoric population from CAALA-329: II. Degenerative disease. *American Journal of Physical Anthropology*, 83(1), 83–94. <https://doi.org/10.1002/ajpa.1330830110>
- Jurmain, R. D., & Kilgore, L. (1995). Skeletal evidence of osteoarthritis: A palaeopathological perspective. *Annals of the Rheumatic Diseases*, 54(6), 443–450. <https://doi.org/10.1136/ard.54.6.443>
- Katz, D., & Suchey, J. M. (1986). Age determination of the male os pubis. *American Journal of Physical Anthropology*, 69(4), 427–435. <https://doi.org/10.1002/ajpa.1330690402>
- Kelley, S. R., & Tallman, S. D. (2022). Population-Inclusive Assigned-Sex-at-Birth Estimation from Skull Computed Tomography Scans. *Forensic Sciences*, 2(2), 321–348. <https://doi.org/10.3390/forensicsci2020024>
- Klara, K., Collins, J. E., Gurary, E., Elman, S. A., Stenquist, D. S., Losina, E., & Katz, J. N. (2016). Reliability and accuracy of cross-sectional radiographic assessment of severe knee osteoarthritis: role of training and experience. *The Journal of Rheumatology*, 43(7), 1421–1426. <https://doi.org/10.3899/jrheum.151300>
- Kochhar, A. S., Sidhu, M. S., Prabhakar, M., Bhasin, R., Kochhar, G. K., Dadlani, H., Spagnuolo, G., & Mehta, V. V. (2021). Intra- and Interobserver reliability of bone volume estimation using OSIRIX software in patients with cleft lip and palate using cone beam computed tomography. *Dentistry Journal*, 9(2), 1–12. <https://doi.org/10.3390/dj9020014>
- Komar, D. (1998). Decay rates in a cold climate region: A review of cases involving advanced decomposition from the medical examiner's office in Edmonton, Alberta. *Journal of Forensic Sciences*, 43(1), 57–61. <https://doi.org/10.1520/jfs16090j>
- Komar, D. (2003). Lessons from Srebrenica: The contributions and limitations of physical anthropology in identifying victims of war crimes. *Journal of Forensic Sciences*, 48(4), 1–4. <https://doi.org/10.1520/jfs2002153>
- Kurenov, S. N., Ionita, C., Sammons, D., & Demmy, T. L. (2015). Three-dimensional printing to facilitate anatomic study, device development, simulation, and Planning in Thoracic Surgery. *The Journal of Thoracic and Cardiovascular Surgery*, 149(4), P973–979.E1. <https://doi.org/10.1016/j.jtcvs.2014.12.059>

- Landi, F., & O'Higgins, P. (2019). Applying Geometric Morphometrics to Digital Reconstruction and Anatomical Investigation. *Advances in Experimental Medicine and Biology*, 1171, 55–71. [https://doi.org/10.1007/978-3-030-24281-7\\_6](https://doi.org/10.1007/978-3-030-24281-7_6)
- Landis, J. R., & Koch, G. G. (1977). The measurement of observer agreement for categorical data. *Biometrics*, 33(1), 159. <https://doi.org/10.2307/2529310>
- Langley, N. R., Jantz, L. M., Ousley, S. D., Jantz, R. L., & Milner, G. (2016). DATA COLLECTION PROCEDURES FOR FORENSIC SKELETAL MATERIAL . Forensic Anthropology Center Department of Anthropology The University of Tennessee Knoxville, Tennessee, 2.0.
- Listi, G. A., & Manhein, M. H. (2012). The Use of Vertebral Osteoarthritis and Osteophytosis in Age Estimation. *Journal of Forensic Sciences*, 57(6), 1537–1540. <https://doi.org/10.1111/j.1556-4029.2012.02152.x>
- Lovejoy, C. O. (1985) Dental wear in the Libben population: Its functional pattern and role in determination of adult skeletal age at death. *American Journal of Physical Anthropology*, 68, 47–56.
- Lovejoy, C. O., Meindl, R. S., Pryzbeck, T. R., & Mensforth, R. P. (1985). Chronological metamorphosis of the auricular surface of the ilium: A new method for the determination of adult skeletal age at death. *American Journal of Physical Anthropology*, 68(1), 15–28. <https://doi.org/10.1002/ajpa.1330680103>
- Mann, R. W., R. L. Jantz, W. M. Bass, and P. S. Willey (1991) Maxillary suture obliteration: A visual method for estimating skeletal age. *Journal of Forensic Sciences* 36, 781–791.
- Malone, C. A., Sauer, N. J., & Fenton, T. W. (2011). A radiographic assessment of pediatric fracture healing and time since injury. *Journal of Forensic Sciences*, 56(5), 1123–1130. <https://doi.org/10.1111/j.1556-4029.2011.01820.x>
- Martel-Pelletier, J. (1999). Pathophysiology of osteoarthritis. *Osteoarthritis and Cartilage*, 7(4), 371–373. <https://doi.org/10.1053/joca.1998.0214>
- Mathiessen, A., Cimmino, M. A., Hammer, H. B., Haugen, I. K., Iagnocco, A., & Conaghan, P. G. (2016). Imaging of osteoarthritis (OA): What is new? *Best Practice & Research Clinical Rheumatology*, 30(4), 653–669. <https://doi.org/10.1016/j.berh.2016.09.007>
- McCulloch, K., Litherland, G. J., & Rai, T. S. (2017). Cellular senescence in osteoarthritis pathology. *Aging Cell*, 16(2), 210–218. <https://doi.org/10.1111/accel.12562>
- Meindl, R. S., & Lovejoy, C. O. (1985). Ectocranial suture closure: A revised method for the determination of skeletal age at death based on the lateral-anterior sutures.

- American Journal of Physical Anthropology*, 68(1), 57–66.  
<https://doi.org/10.1002/ajpa.1330680106>
- Mertens, K., Mespreuve, M., & Vanhoenacker, F. M. (2023). Lunotriquetral Coalition. *Seminars in Musculoskeletal Radiology*, 27(03), 378–380. <https://doi.org/10.1055/s-0043-1766108>
- Meshmixer | Fusion | Autodesk App Store*. (n.d.).  
<https://apps.autodesk.com/FUSION/en/Detail/HelpDoc?appId=4108920185261935100&appLang=en&os=Win64#:~:text=Fusion%20now%20contains%20many%20of,supported%20by%20Autodesk%20moving%20forward.>
- Mincer, H. H., E. F. Harris, and H. E. Berryman (1993) The A.B.F.O. study of third molar development and its use as an estimator of chronological age. *Journal of Forensic Sciences* 38(2), 379–390.
- Moorrees, C. F. A., E. A. Fanning, and E. E. Hunt (1963) Age variation of formation stages for ten permanent teeth. *Journal of Dental Research*, 42(6), 1490–1502.
- Obertová, Z., Stewart, A., & Cattaneo, C. (2020). *Statistics and probability in forensic anthropology*. Academic Press.
- Ortner, D. J. (2003). *Identification of pathological conditions in human skeletal remains*. Academic Press.
- Paramasivam, V., Sindhu, Singh, G., & Santhanakrishnan, S. (2020). 3D printing of human anatomical models for preoperative surgical planning. *Procedia Manufacturing*, 48, 684–690. <https://doi.org/10.1016/j.promfg.2020.05.100>
- Pokines, J. T., Symes, S. A., & L'Abbé, E. N. (2022). *Manual of Forensic Taphonomy*. CRC Press.
- Rahim, M., Norouzi, A., Rehman, A., & Saba, T. (2017). 3D bones segmentation based on CT images visualization. *Biomedical Research*, 28(8), 3641–3644.  
<https://www.biomedres.info/biomedical-research/3d-bones-segmentation-based-on-ct-images-visualization.pdf>
- Ritt, M. J. P. F., Maas, M., & Bos, K. E. (2001). Minnaar type 1 symptomatic LUNOTRIQUETRAL coalition: A report of nine patients. *The Journal of Hand Surgery*, 26(2), 261–270. <https://doi.org/10.1053/jhsu.2001.21520>
- Ross, A. H., & Pilloud, M. (2021). The need to incorporate human variation and evolutionary theory in forensic anthropology: A call for reform. *American Journal of Physical Anthropology*, 176(4), 672–683. <https://doi.org/10.1002/ajpa.24384>

- Rosset, A., Spadola, L., & Ratib, O. (2004). Osirix: An open-source software for navigating in multidimensional dicom images. *Journal of Digital Imaging, 17*(3), 205–216. <https://doi.org/10.1007/s10278-004-1014-6>
- Sanchez, A., Tallman, S. D., Winburn, A. P., & Stefanik, J. (2021). The effects of orthopedic pathological conditions and systemic diseases on the prevalence of hip osteoarthritis in Modern African- and European-Americans. *HOMO: Journal of Comparative Human Biology, 72*(3), 183–203. <https://doi.org/10.1127/homo/2021/1329>
- Scheuer, L., & Black, S. M. (2004). Juvenile skeleton. Elsevier Academic Press. Sezer, I., Illeez, O. G., Tuna, S. D., & Balci, N. (2010). The relationship between knee osteoarthritis and osteoporosis. *The Eurasian Journal of Medicine, 42*(3), 124–127. <https://doi.org/10.5152/eajm.2010.35>
- Shane Anderson, A., & Loeser, R. F. (2010). Why is osteoarthritis an age-related disease? *Best Practice & Research Clinical Rheumatology, 24*(1), 15–26. <https://doi.org/10.1016/j.berh.2009.08.006>
- Siebelt, M., Korthagen, N., Wei, W., Groen, H., Bastiaansen-Jenniskens, Y., Müller, C., Waarsing, J. H., de Jong, M., & Weinans, H. (2015). Triamcinolone acetonide activates an anti-inflammatory and folate receptor–positive macrophage that prevents osteophytosis in vivo. *Arthritis Research & Therapy, 17*(1). <https://doi.org/10.1186/s13075-015-0865-1>
- Snodgrass, J. J. (2004). Sex Differences and Aging of the Vertebral Column. *Journal of Forensic Sciences, 49*(3), 1–6. <https://doi.org/10.1520/jfs2003198>
- Spiros, M., Nakhaeizadeh, S., Thompson, T., Morgan, R., Olsson, V., Berivoe, A., Hefner, J., & Arvidsson, M. (2022). Using eye-tracking technology to quantify the effect of experience and education on forensic anthropological analyses. *Forensic Anthropology, 6*(1), 25–35. <https://doi.org/10.5744/fa.2022.0001>
- Stachowiak, G. W., Wolski, M., Woloszynski, T., & Podsiadlo, P. (2016). Detection and prediction of osteoarthritis in knee and hand joints based on the X-ray image analysis. *Biosurface and Biotribology, 2*(4), 162–172. <https://doi.org/10.1016/j.bsbt.2016.11.004>
- Strasheim, A. N., Winburn, A. P., & Stock, M. K. (2023). Utility of osteoarthritis as an indicator of age in human skeletal remains: Validating the Winburn and stock (2019) method. *Forensic Sciences, 3*(2), 205–230. <https://doi.org/10.3390/forensicsci3020016>
- Tarantino, U., Celi, M., Rao, C., Feola, M., Cerocchi, I., Gasbarra, E., Ferlosio, A., & Orlandi, A. (2014). Hip osteoarthritis and osteoporosis: Clinical and

- histomorphometric considerations. *International Journal of Endocrinology*, 2014, 1–5. <https://doi.org/10.1155/2014/372021>
- Udupa, J. K., Hung, H.-M., & Chuang, K.-S. (1991). Surface and volume rendering in three-dimensional imaging: A Comparison. *Journal of Digital Imaging*, 4(3), 159–168. <https://doi.org/10.1007/bf03168161>
- Verma, M., Verma, N., Sharma, R., & Sharma, A. (2019). Dental age estimation methods in adult dentitions: An overview. *Journal of Forensic Dental Sciences*, 11(2), 57. [https://doi.org/10.4103/jfo.jfds\\_64\\_19](https://doi.org/10.4103/jfo.jfds_64_19)
- Vidoli, G. M. (2022). The New Mexico Decedent Image Database: Demographics, life, and the body (<https://nmdid.unm.edu/>). *American Journal of Biological Anthropology*, 179(2), 331–332. <https://doi.org/10.1002/ajpa.24584>
- Waldron, T. (2009). *Palaeopathology*. Cambridge University Press.
- Wallace, I. J., Worthington, S., Felson, D. T., Jurmain, R. D., Wren, K. T., Maijanen, H., Woods, R. J., & Lieberman, D. E. (2017). Knee osteoarthritis has doubled in prevalence since the mid-20th century. *Proceedings of the National Academy of Sciences of the United States of America*, 114(35), 9332–9336. <https://doi.org/10.1073/pnas.1703856114>
- Watanabe, S., & Terazawa, K. (2006). Age estimation from the degree of osteophyte formation of vertebral columns in Japanese. *Legal Medicine*, 8(3), 156–160. <https://doi.org/10.1016/j.legalmed.2006.01.001>
- Webb, P. A. and J. M. Suchey (1985) Epiphyseal union of the anterior iliac crest and medial clavicle in a modern multiracial sample of American males and females. *American Journal of Physical Anthropology* 68, 457–466.
- Weber, G. W., & Bookstein, F. L. (2017). *Virtual anthropology: A guide to a new interdisciplinary field*. Springer.
- Wemrell, M., Merlo, J., Mulinari, S., & Hornborg, A. (2016). Contemporary Epidemiology: A Review of Critical Discussions Within the Discipline and A Call for Further Dialogue with Social Theory. *Sociology Compass*, 10(2), 153–171. <https://doi.org/10.1111/soc4.12345>
- White, T. D., Black, M. T., & Folkens, P. A. (2012). *Human osteology*. Academic Press.
- Winburn, A. P., & Stock, M. K. (2019). Reconsidering osteoarthritis as a skeletal indicator of age at death. *American Journal of Physical Anthropology*, 170(3), 459–473. <https://doi.org/10.1002/ajpa.23914>

**CURRICULUM VITAE**

